The role of Cadherin 4 in the assembly of retinal circuits

Aline Giselle Rangel Olguin

Master of Science
Department of Physiology
McGill University, Montreal, Quebec, Canada
April 2020

A thesis submitted to McGill University in partial fulfillment
of the requirements for the degree of Master of Science.

Table of Contents

Abstract

Neurons grow axons and dendrites into target regions where they face hundreds of proximate potential synaptic partners but connect with only a select few. This selectivity is critical for wiring patterns and circuit computations but how it arises is unclear. In the retina, a specialized neuropil called the inner plexiform layer (IPL) organizes the processes of ~40 types of retinal ganglion cells (RGCs) and their ~100 types of interneuron inputs. The IPL is multi-layered, each sublayer enriches the processes of interneuron-RGC partners and is critical for the assembly of feature detecting retinal circuits. Previous work indicates that members of the cadherin superfamily (Cdh) play a crucial role in layer-specific targeting. In this thesis, I show that Cdhs are expressed in distinct patterns across RGC subtypes and start the characterization of Cdh4, also known as retina Cdh. Using genetically encoded markers I show that Cdh4 expression is restricted to interneurons and RGCs that project to upper layers of the IPL, and horizontal cells. These anatomical studies suggest that Cdh4 targets neurons to the OFF regions of the IPL. Taken together, this thesis supports the idea that neurons might use a Cdh code to position their neuropil to achieve synapse selectivity and the existence of an adhesive code.

Résumé

Les neurones développent leurs axones et leurs dendrites vers des régions où ils trouvent des centaines de partenaires synaptiques potentiels mais ne se connectent qu'à quelques privilégiés. Cette sélectivité est essentielle pour établir des motifs de connexion fonctionnels, mais la façon dont se produisent est encore inconnue. Dans la rétine, un neuropile spécialisé appelé couche de plexiforme interne (CPI) organise les neurites de ~ 40 types de cellules ganglionnaires (CG) et leurs ~ 100 types d'interneurones constituent leurs entré d'information neuronale. Le CPI est une structure à 5 couches, où chaque couche est enrichie pour certaines pairs d'interneurone-CG. Cette organisation est essentielle pour l'assemblage des circuits rétiniens qui détectent des caractéristiques visuelles. Des études antérieures indiquent que les membres de la superfamille des cadhérines (Cdh) jouent un rôle crucial en dirigeant les dendrites vers des couches spécifiques de le CPI. Dans cette thèse, je démontre que les Cdhs ont des motifs d'expression distinct parmi les types de CGs et débute la caractérisation de Cdh4, également connue sous le nom de cadhérine rétinienne. En utilisant des marqueurs génétiquement codés, je montre que l'expression de Cdh4 est limitée aux interneurones et aux RGC qui se projettent vers les couches supérieures de la CPI, et les cellules horizontales. Ces études anatomiques suggèrent que Cdh4 cible les neurones vers la région OFF de la CPI. Dans l'ensemble, cette thèse soutient la possibilité que les neurones forment des synapses sélectives en utilisant un code Cdhs pour positionner leurs neurites et qu'il existe un code adhésif.

Acknowledgements

I would like to thank to all the people that guide me, helped me and supported me during my studies. First, I want to thank my supervisor Dr. Krishnaswamy for his guidance, patience and incredible ideas in the past two years that resulted in the satisfactory culmination of this thesis. His incredible mentoring and enthusiasm for science has been key in my development as a scientist. Thanks to my amazing lab fellows that make the lab a welcoming place and who helped me through this project. Specially for those incredible talks at lunch. I would also like to thank my family and friends for all their support along this Masters. A special thanks to Ariel for always cheer me when I needed it and push me to be better in every sense. Finally, I would like to thank Ellis Coper, Stuart Trenholm, Edward Ruthazer and Gil Bub for serving on my committee and as mentors.

Contribution of Authors

The author of this thesis performed the bioinformatic analysis and experiments in this work. This includes scRNA-seq data analysis in R, immunohistology, imaging, injections, preparing figures and writing this thesis. This thesis was revised by Dr. Arjun Krishnaswamy.

1. Introduction

Billions of neurons in our brains form complex neural circuits which give us our ability to perform tasks such as cognitive and sensory processing. Each circuit connects specific combinations of neuron cell types so they can work together to perform unique computations. These circuits are packed and entangled within the skull with their synapses separated from each other at a micrometer scale. Despite this arrangement, they maintain their own specialized function segregated from their neighbors. How neurons discern among equally proximate neurons is not altogether clear but they overcome this problem and wire specifically only with a selected few (Sanes and Yamagata, 1999; Williams et al., 2010; Koropouli and Kolodkin, 2014).

One idea is that synaptic neuronal partners are genetically pre-programed to synapse, a hypothesis termed chemoaffinity which arose from pioneering studies by John Langley and Roger Sperry (JN., 1892; Sperry, 1943). This hypothesis predicts that each axon bore ligands that matched receptors on targets, contact between these two neurons formed intercellular ligand-receptor complexes which then initiated synaptogenesis processes. Years later, Sperry and Langley's chemical matchmakers were found to belong to large families of cell adhesion molecules expressed in both synaptic partners, whose properties make them adhere tightly to each other (Sanes and Yamagata, 2009; Zipursky and Sanes, 2010; Lefebvre et al., 2015). Yet, the number of recognition molecules encoded by the genome is under the amount necessary to wire all the neurons in the nervous system.

To reduce the complexity and number of unique molecules for synaptic specificity, a prominent idea is that the same molecule can be used to wire different neurons if their processes

are separated by developmental time or anatomical space. The latter scenario can be found in virtually every complex nervous tissue –processes are organized into neuropil layers, or laminae, which bear a pool of potential partners for an incoming axon (Sanes and Yamagata, 1999; Oberst et al., 2019). But how do laminae arise? How does a neuron find its appropriate lamina? What are the factors that direct this matching? And what are the functional consequences of laminar choice for circuit function?

The retina is an excellent platform for the study of circuit development to answer these questions (Fuerst et al., 2009; Sanes and Zipursky, 2010; Matsuoka et al., 2011b; Wei et al., 2011; Lefebvre et al., 2012; Sun et al., 2013; Duan et al., 2014; Krishnaswamy et al., 2015). This thin sheet of neuronal tissue located at the back of the eye contains many of the anatomical, cellular and molecular features of higher circuits in the brain but is considerably more tractable. A plethora of efforts from many research groups have taught us many aspects of the retina: single-cell RNA sequencing (scRNA-seq) studies have provided a complete molecular taxonomy of retinal cell types (Macosko et al., 2015; Shekhar et al., 2016; Rheaume et al., 2018); each cell-type can be marked and manipulated using a nearly complete catalogue of mouse lines available in public repositories; 60 years of elegant studies on retinal computations have provided a rich stimulus set with which to test the functional consequences of laminar choice; and recent work from our lab (Duan et al., 2014; Krishnaswamy et al., 2015) has provided rapid ways to map connectivity among neuron types. The similarities of the retina with the brain, its anatomically accessibility and recent advances in understanding the retina makes it incredible tractable to answer how synapse specificity arises in this system.

The goal of this project has been to understand better the molecular mechanisms that mediate layering and the role of such layering in synapse selectivity. In the following sections I provide background of how the retina is organized, its circuits, cell types, development and molecules that play a role in assembling neuronal circuits with special focus on cadherins.

1.1. The general plan of the retina

The retina is a part of the central nervous system (CNS) composed of six principal retinal cell types: photoreceptors (PRs), three interneuron types, projection neurons called retinal ganglion cells (RGCs) and Müller glia (Fig. 1A). Every retinal circuit begins with a PR, which detects photons and signals their presence to two types of interneurons, bipolar cells (BCs) and horizontal cells (HCs). BCs in turn synapse with the amacrine cell (AC) and HC interneurons, and RGCs (Masland, 2012a; Sanes and Masland, 2015; Seabrook et al., 2017); HCs modulate PR-BCs synapses. Lastly, RGCs integrate the excitatory input from BCs with inhibitory AC input and send this message to the brain for further analysis (Seabrook et al., 2017). Synapses among a subset of the ~150 BC, RGC, and AC types result in several parallel circuits, each detects a specific aspect of the visual scene such as motion, edges, and so on (Gollisch and Meister, 2010). These neuron somata are organized in three nuclear layers: an outer layer containing PRs (ONL), an inner layer containing interneurons and glia (INL) and a ganglion cell layer (GCL) containing RGCs and some displaced ACs (dACs) (Gollisch and Meister, 2010). These nuclear layers are separated by two specialized plexiform layers: an outer plexiform layer (OPL), a neuropil in which the processes of PRs, HCs and BCs intermingle to form synapses (Sanes and Masland, 2015); and the inner plexiform layer (IPL), a neuropil that organizes wiring of the ~40 feature-detecting neural circuits formed by BCs

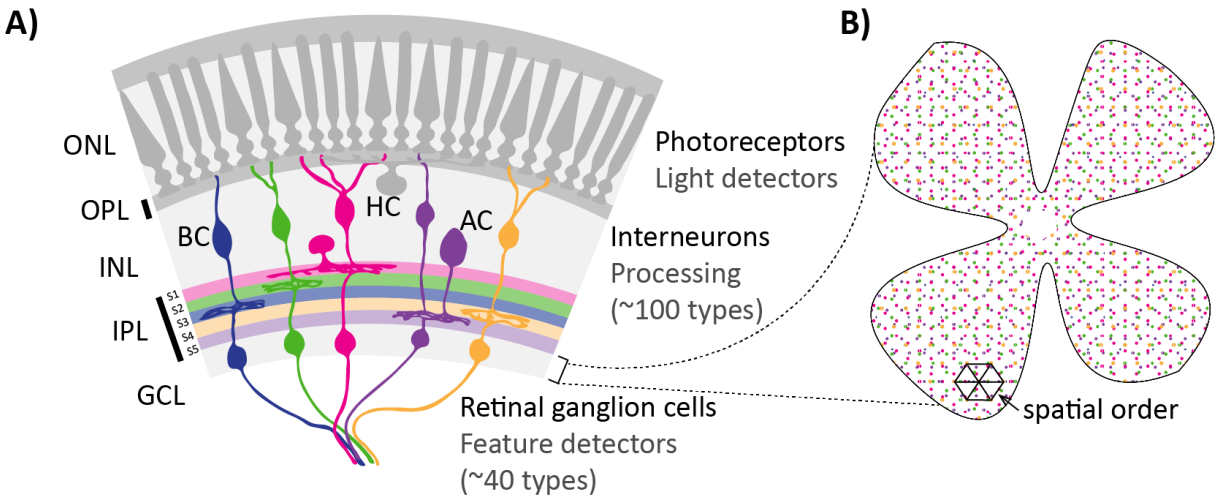

Figure 1. Retina organization. A: Laminar organization, nuclear layers are separated by two specialized neuropil layers. **B**: Lateral organization, neurons follow a stereotyped intracellular spacing and density distribution across the retina called mosaics. Hexagon exemplifies spacing for yellow cells. BC, bipolar cell; AC, amacrine cell; HC, horizontal cell; ONL, outer nuclear layer; OPL, outer plexiform layer; INL, inner nuclear layer; IPL, inner plexiform layer; S1-S5, sublamina1-5.

that synapse with RGCs and ACs (Demb and Singer, 2015; Baden et al., 2016). Such connected RGC-interneuron subsets are organized into 5-10 possible IPL sublaminae, suggesting that developing neurons choose one of these layers to wire selectively (Masland, 2012a).

1.2. Retinal cell types

1.2.1. Photoreceptors

PRs provide the first contact of the CNS with the outside visual world by converting light into an electrical signal. The vertebrate retina contains two types of PRs: cones that provide the color daylight action and rods for starlight vision. Each PR type is tuned to a specific light wavelength and amplifies photon detection signals that are conveyed to interneurons for further information processing (Lolley and Lee, 1990). In the mouse retina, rods account for 97% of retinal PRs and are sensitive to single photons with a maximum absorption at 500nm (Carter-Dawson and Lavail,

1979; Lolley and Lee, 1990; Nikonov et al., 2006). Rods are continuously activated by their ion channels, causing a steady release of glutamate to signal their postsynaptic interneurons that the environment is dark, known as “dark current” (Fu and Yau, 2007). This signal ceases when the absorption of a single photon triggers the phototransduction cascade as follow: 1) Rhodopsin becomes active when a photon isomerizes its chromophore; 2) active Rh catalyzes the replacement of GDP for GTP in the G-protein transducin; 3) transducin-GTP actives the cCMP phosphodiesterase (PDE); 4) PDE hydrolyze cGMP; 5) low levels of cGMP allows cGMP-gated ion channels to close; 6) inward current of Na+, Ca+, and Mg 2+ is interrupted; and 7) the membrane hyperpolarizes which stops glutamate release (Lagnado and Baylor, 1992). This drop of glutamate release from rod PRs is interpreted as absence of darkness by its postsynaptic partners (Lolley and Lee, 1990; Fu and Yau, 2007). Cones, which account for the remaining 3% of retinal PRs, provide temporal resolution and, in mice, co-express two pigments in them for color vision: S- and M-cone pigments, with maximal spectral sensitivity at 360 and 508 nm, respectively (Nikonov et al., 2006). M-pigment is expressed in a decreasing gradient from dorsal to ventral while S-pigment is constant (Carter-Dawson and Lavail, 1979; Applebury et al., 2000; Fu and Yau, 2007).

1.2.2 Bipolar Cells

BCs link the outer and inner retina by collecting input from PRs at their dendrites in the OPL and delivering it to every other type of retinal neuron via their axons in the IPL. They separate the tuned input from PRs into different channels to encode the first elementary operations of the visual system for properties such as light-onset (ON) versus light-offset (OFF) responses, speed, contrast, temporal profile and chromatic composition (Euler et al., 2014). In mammals, BCs have been classified as ON and OFF cone BCs (CBs), and rod BCs (RBs) according to the number of

cones and rods contacted (see below in circuits for ON and OFF differences) (Sterling et al., 1995). These, in turn, haven been subdivided based on morphology and molecular identity into ~15 subtypes (Shekhar et al., 2016) whose output signals are the 'building blocks' for the representation of visual features performed by RGCs (Euler et al., 2014). Thus, BCs features derive from the connection with their synaptic partners and intrinsic properties.

1.2.3 Horizontal cells

Lateral interactions modulate how visual information flows in the vertical axis of the retinal. HCs facilitate pathways that underlie color opponency and contrast enhancement (Twig et al., 2003). Additionally, HCs provide feed forward signals to CBs and feedback to cones, resulting in regulation of center-surround receptive field (RF) organization (Thoreson and Mangel, 2012). Briefly, center modulation of CBs is regulated by cones connecting directly to them, and surround inputs mediated by inhibition from lateral HC connections that in turn are activated by cones in the surround (Yang and Wu, 1991). In most mammals HCs are divided morphologically into axon-bearing and axon-less subtypes. HCs axons-terminus mainly connect with rods and their dendritic arbors predominantly to cones (Zhang et al., 2006b, 2006a). HCs subtypes seems to be slightly linked to relative cone/rod ratio in the retina. In mammals, where rods are extremely dominant, like the mouse retina, only axon-bearing HCs are present (Peichl and González-Soriano, 1994; Ahnelt and Kolb, 2000).

1.2.4 Amacrine cells

HCs in the OPL are the first inhibitory network in the retina visual pathway. The second inhibitory network is created by ACs in the IPL where they modulate visual signals of: BC synaptic terminals

via presynaptic (feedback) excitation; RGC dendrites via postsynaptic (feedforward) inhibition; and lateral inhibitory synapses onto other ACs (MacNeil and Masland, 1998; Helmstaedter et al., 2013; Diamond, 2017). ACs constitute the most diverse cell type in the retina with approximately 50 different subtypes in mice with unique patterns sizes, functions, and stratifications into the IPL (Masland, 2012b; Diamond, 2017). The large diversity in ACs has been linked to provide complex spatiotemporal information that endow RGCs with their subtle feature recognition of the different representation of the visual world. Most ACs possess no axon and have been classified morphologically as wide, medium, and narrow-field (MacNeil and Masland, 1998; Diamond, 2017). Wide and medium-field ACs are GABAergic, and narrow-field ACs are glycinergic; with all of them also releasing a second neurotransmitter (glutamate, acetylcholine, dopamine, peptide, etc.) (Werblin, 2011; Masland, 2012b; Diamond, 2017).

1.2.5 Retinal Ganglion Cells

RGCs integrate convergent visual input from ACs and BCs to detect specific visual features. Detected features are encoded as a series of action potentials and sent for further analysis to the retinorecipient regions in the brain via the optic nerve (Shi et al., 2019). The regions with the major RGC input are the lateral geniculate nucleus, superior colliculus and midbrain pretectal nuclei (Martersteck et al., 2017). In the mouse retina ~ 40 different types of RGCs have been identified to date based on morphology, physiology and gene expression (Sanes and Masland, 2015; Baden et al., 2016; Rheaume et al., 2018).

1.3 Retinal organization

1.3.1 Laminar organization

In the vertebrate retina, appropriate formation of parallel circuits relies on synapse specificity among different retinal neurons. Proper circuit assembly ensures their ability to process visual information and an accurate perception (Zipursky and Sanes, 2010). The IPL contains a highly compacted number of these synapses among RGCs, ACs and BCs (Fig. 1A). Cajal was one of the first ones to recognize the layered organization of the retina. In his pictures he shows the relationship of cell type diversity and their arbors into different depths of the IPL (y Cajal Santiago Ramón, 1972; Sanes and Zipursky, 2010). Given this complexity, Cajal used Golgi methods to subdivide the IPL into approximately five sublaminae (S1-S5). This organization can been seen in virtually all vertebrates, which allows a comparative classification of BCs, ACs, and RGCs based on the sublaminar stratification of their processes (Karten and Brecha, 1983).

The IPL sublaminae can be easily revealed by immunostaining for marker proteins, present on various retinal types. For example, S2 and S4 can be defined by labeling the vesicular acetylcholine transporter (vAChT) on cholinergic terminals of ACs; S1, S3 and S5 can be marked with antibodies directed against L-glutamate decarboxylase (GAD) contained by GABAergic ACs (Karten and Brecha, 1983); S3 by labeling the glutamate vesicular transporter 3 (Vglut3) from glutaminergic ACs (Johnson et al., 2004); and S1 using markers against TH from dopaminergic cells (Ballesta et al., 1984). Further subdivision is possible and nearly 10-15 sublaminae have been described based on the pattern of other histochemical stains (Karten and Brecha, 1983; Zhang et al., 2005). The existence of this layering agrees with the idea of neuron connections organized to

split the different information channels that process different visual features. In addition, the existences of continuous layers across the lateral axis of the IPL is given by a lateral organization of retinal neurons of the same type.

1.3.2 Lateral Organization (Mosaics)

Each retinal neuron type has its own intrinsic spacing between neighboring cells of its same type across the lateral axis (Fig. 1B) (Reese and Galli-Resta, 2002). Local intracellular interaction and repulsion during development forces apart dendritic arbors belonging to the same kind of cell. Collectively, this force spaces neurons of the same type into a triangular lattices called mosaics. (Rodieck and Marshak, 1992; Cook and Chalupa, 2000). Experimentally, an easy way to validate candidate cell-type markers is by determining whether marked cells are arranged in a mosaic (Sanes and Masland, 2015).

RFs of the same cell type organized in a mosaic tile the visual space for the detection of a specific feature (Field et al., 2007). These RFs are formed by either an ON or OFF antagonistic center-surround (Turner et al., 2018). For example, an ON-center cell becomes active with increments of light in the center of its RF or inhibited with increments of light in its surround; conversely, OFF-center cells activate with decrements of light in the center of their RF and inhibited with decrements of light in their surround. RF center-surround of ACs and RGCs are given by their connections to ON-center and OFF-center BCs (see section 1.2.3) and are a key component of many retinal circuits as described in the next section.

1.4 Retinal circuits

1.4.1 ON vs OFF responses

Sensitivity to light onset and light offset originate in BCs (Werblin and Dowling, 1969; Chalupa and Günhan, 2004). In the dark, PRs release glutamate onto both ON and OFF BCs. On OFF BCs it binds to ionotropic glutamate receptors which depolarize these cells; Glutamate release onto ON BCs activates type 6 metabotropic glutamate receptors (mGluR6) which causes closure of non-selective, cation conducting TRPM1 channels and hyperpolarizes these cells (Koike et al., 2010b, 2010a; Euler et al., 2014). Light hyperpolarizes PRs, which decreases their glutamate release and inverts this signal. The separation of ON and OFF responses is maintained in the IPL: OFF BCs grow their axons in S1 to upper S3 (uS3) while ON BCs grow their axons in lower S3 to S5 (Euler et al., 2014). Synapses formed by these BCs on resident AC and RGCs cause these cells to become sensitive to light onset or offset (Chalupa and Günhan, 2004). Crosstalk between layers is minimal, however, some glycinergic ACs collect ON or OFF input and deliver it to retinal neurons that prefer opposite changes in light intensity. This circuit motif, called crossover inhibition, is critical for linearizing retinal responses to changes in brightness and is central to the rod circuitry that permits scotopic vision (Molnar et al., 2009). Thus, intrinsic BCs properties result in one of the major splits of visual information in the retina to detect brightening or dimming.

1.4.2 Direction selectivity

Detection of image motion direction in the retina is performed by direction selective RGCs (DSGCs) that respond strongly to visual motion and speed in one particular direction (ventral, dorsal, temporal, nasal) and weakly to the opposite (null) direction (Barlow and Levick, 1965). To

do so, DSGCs integrate BCs excitation with inhibition received from starburst ACs (SACs) positioned in the preferred direction (Briggman et al., 2011). An object moving in the preferred direction across the DSGC RF recruit BC excitation before they recruit SAC inhibition; conversely, moving objects in the null direction recruit SAC inhibition before they can recruit BC excitation which silences DSGC spiking (Yoshida et al., 2001). Thus, SAC inhibition has been described as a key component to dictate DSGC preferences towards an object moving in a specific direction.

1.4.3 Object motion sensitivity

Object motion selective (OMS) circuits discern the motion of a small dark object from its background, even if this background is moving (Ölveczky et al., 2007). In mice, OMS RGCs are called W3B-RGCs which receive sluggish excitation in their RF center from BCs and VGlut3-ACs (VG3-ACs), and speedy inhibition from wide-field TH-ACs that fire action potentials (Lee et al., 2014; Kim et al., 2015; Krishnaswamy et al., 2015; Hsiang et al., 2017; Kim and Kerschensteiner, 2017). Background, or global, motion activates both center and surround pathways whose sluggish and speedy time-courses causes their signals to cancel out, silencing W3B-RGCs. When center-motion differs from the surround, such as happens with a moving object, the center excitation appears out of synch with the surround and results in firing (Baccus et al., 2008). Thus, W3-RGCs respond to motion at the center of their RF, but only if the wider surround moves with a different speed.

1.5 Retinal development

1.5.1 Cell differentiation

Retinal development deals with the production of the proper ratio of cell types, migration of somas to right layers, differentiation and targeting to form synaptic connections. These steps are highly conserved across vertebrates, including the major cell types used to assemble the retina (six types of neurons and one glia cell type) (Centanin and Wittbrodt, 2014). The richness in cell types of the retina derives from multipotential precursors called retinal progenitor cells (RPCs) (Centanin and Wittbrodt, 2014). In the mouse, retinal neurogenesis starts at embryonic day 8 (E8), after the optic cup has formed, and continues until postnatal day 11 (P11) (Young, 1985). Here, RPCs positioned in the apical side of the developing retina and migrate radially to the basal side to differentiate in a stereotyped order (Centanin and Wittbrodt, 2014). It has been described that RPCs give rise to all the retinal cells types based on series of stages they undergo in which their competence to respond to environmental cues changes across time, restricting their differentiation to one, or few, specific cell types in each stage, known as 'competence model' (Cepko et al., 1996). RGCs (E8-E17) and HCs (E10-P4) differentiate first, followed by overlapping waves of differentiating cones (E10-E18), ACs (E8-P5), BCs (E17-P6), then Müller glia cells (E14-P8) and rods (E13-P11) (Carter-Dawson and Lavail, 1979; Young, 1985; Marquardt and Gruss, 2002; Voinescu et al., 2009). As RGCs, BCs, and ACs retinal neurons differentiate they project their axon and dendrites into just one or perhaps two of the ~5 IPL sublayers and subsequently form connections with their already available partner or wait for them to arrive.

1.5.2 Migration

Newborn neurons migrate to complete their differentiation, and in the retina, this process forms the nuclear layers: ONL, INL and GCL. Each principal type migrates to a different location within these nuclear layers. In the INL, for example, HCs comprise the outermost layer of somata, BCs comprise the middle and ACs occupy the innermost layers. As cells differentiate they use different migration strategies to find their final position: radially (perpendicular to basal-apical axis), tangential (parallel to basal-apical axis) or/and multipolar (any direction) (Amini et al., 2018). Signals that guide cells have been found on the extracellular matrix and on neighboring cells. For example, laminins are enriched in the inner limiting membrane (ILM) that limits the retina basally and direct RGCs through the β1- Integrin laminin receptor to form a single-cell GCL. When mutated RGCs from clusters beyond the ILM (Riccomagno et al., 2014).

1.5.3 IPL formation

The processes of the first differentiated retinal neurons form a proto-IPL that scaffolds the projections of later-born cells (Riccomagno et al., 2014). Here, repulsive and attractive cues are critical for this phenomenon and the appearance of a mature IPL.

1.5.3.1 Repulsive molecular cues define nuclear and neuropil regions

INL and GCL are well defined layers actively segregated from the IPL by the members of the Semaphorin (Sema) family and their Plexin receptors (Plex). Sem-Plex interactions are known for mediating dendrite and axon guidance, polarization and repulsion (Huber et al., 2003). Semas are either expressed in the plasma membrane or secreted to bind and activate Plex receptors from developing neurites to induce growth cone collapse and repel them from the Sema expressing

substrates (Huber et al., 2003). In the retina, Sema5A and 5B are expressed by neurites localized in the INL during retinal synaptogenesis (P3-P14) (Matsuoka et al., 2013; Zhang et al., 2017) and disappears from these cells by P21. In retinas lacking these Sema-Plex interactions, dendrites and axons not only innervate the IPL but project new processes that from ectopic IPL-like structures in the INL or extend beyond into the ONL (Matsuoka et al., 2011a). Repulsive cues reinforce a pre-existing attraction towards the IPL rather than acting as the sole driver of IPL-directed growth. Such pre-existing attractive cues remain to be unveiled but the atypical cadherin FAT3 could be a potential candidate because its disruption causes processes to extend into the INL like in Plex-Sema mutants (Deans et al., 2011, 3). Thus, a balance between attractive and repulsive cues appears to separate neuronal processes from somas to form well defined plexiform regions.

1.5.3.2 Attractive cues create IPL sublaminae

IPL is formed between birth and eye opening at P12 (Luo and Yau, 2005). Here, dendrites and axons target different sublaminae in the IPL to assemble retinal circuits, but a proto-IPL must be stablished first for subsequent neurons built upon this scaffold. Recent studies from Ray et al., have revealed some sublaminar mechanisms by analyzing the assembly of direction selectivity circuits (see below) in the mouse retina (Ray et al., 2018).

Two population of SACs compose the ON-OFF direction selectivity circuit, one resides in the INL, is sensitive to light offset and projects to S2 (Off-SACs) and the other resides in the GCl, responds to light onset, and projects to S4 (ON-SACs). Both SACs form their respective sublaminae at P0-P1 by creating an initial plexus of contacts among neighboring SACs that extend into the IPL (Ray et al., 2018). Subsequently, their BC and ON-OFF DSGC (ooDSGC) synaptic partners arrive and guided by already stratified SACs target s2 and s4 (Stacy and Wong, 2003; Sun

et al., 2013; Ray et al., 2018). SACs contacts are dependent on the transmembrane protein Megf10, whose loss ablates inter-SACs contacts, and causes diffusion of their projections out of s2 and s4 (Ray et al., 2018). DSGCs and BCs colocalize with these ectopic projections but DSGCs direction selectivity is disrupted, suggesting that partner recruitment is mediated by independent cues from megf10-dependent sublamina formation. Thus, Megf10-based signals are critical for SACs to form an early pair of laminae, which serve as a substrate for their eventual synaptic partners.

Whether each retinal type possesses their own Megf10-like mechanism to establish sublamina or whether this mechanism is unique to SACs is not clear. In the case of the latter, the pair of SAC laminae would act as reference points that later-born neurons could use to position their arbors. The observation that ectopic SAC laminae can recruit the processes of later-arriving neurons favors this possibility.

1.6 Sublamina selection

IPL sublamination is a major determinant of AC and RGC function. For example, in ON-OFF circuits (refer to 1.4.1 above) ON-RGCs and OFF-RGCs arbors are restricted to the inner or outer regions, respectively, where they synapse with the BCs that endow them with their light responsiveness (Masland, 2012a). Recent work suggests that different Cdh are expressed among ON-OFF DSGCs, ON- and OFF- BCs, and ON- and OFF-SACs and direct their processes into S2 and S4 to create circuits that detect the direction of a moving edge.

1.6.1 Cadherin superfamily

The Cdh superfamily is composed of over 80 single-pass transmembrane adhesion molecules. Cdhs receive their names from the calcium-dependent, cadherin motif in their ectodomains (EC) which they use for binding; an intracellular domain (ICD) activates second-messenger systems to transmit binding events to the cell's interior (Takeichi, 1988). Cdhs typically bind in a homophilic fashion but heterophilic interactions, particularly among related isoforms have been described (ie: Cdh8 and 11, 6 and 10,and 9 and 10) (Shimoyama et al., 2000).

1.6.2 Classical cadherins in the brain

Classical Cdhs (type I and II) include members from Cdh1 to Cdh26 (Fig. 2). Five EC repeats and an ICD binding to catenin are a characteristics that define classical Cdhs (Basu et al., 2015).

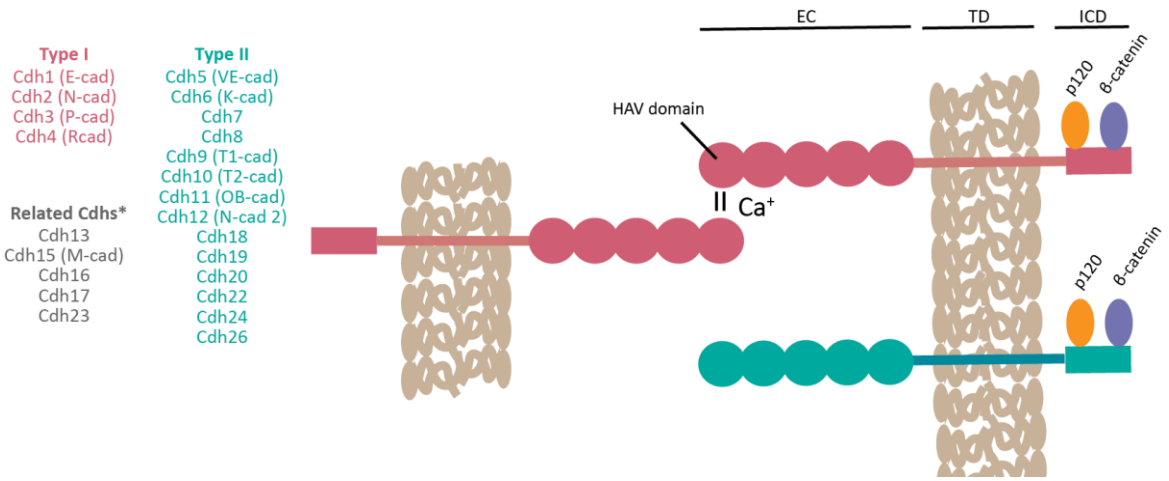

Figure 2. Structure of the classical cadherin protein family. Classical Cdhs contain five extracellular domains (EC), a transmembrane domain (TM) and an intracellular domain (ICD). They use ECs to form calcium-dependent homophilic interactions that signal downstream through their ICD, who activates p120 and β-catenin. Classical Cdhs are subdivided in Type I and II by the presence of a histidine-alanine-valine (HAV) motif in the first EC domain. *Related Cdhs differ structurally: Cdh13, like Type I and Type II Cdhs, contains five EC but contains glycosyl-phosphatidylinositol (GPI) instead of TM and is lacks an ICD. Cdh15, 16, 17 and 23 vary in the number of EC domains. Redrawn with modifications from Basu et al. (2015).

Classical Cdhs are expressed combinatorically In the brain (Suzuki et al., 1997). They localize on synapses, close to the transmitter release site (Yamagata et al, 1995; Fannon and Colman, 1996; Uchida et al., 1996). New studies have led to postulate Cdhs as the molecules that promote synapse formation by bringing together presynaptic and postsynaptic neurons that express the same Cdh isoform (Hatta et al., 1987; Suzuki et al., 1991; Inoue et al., 1998; Miskevich et al., 1998). Suzuki et al., showed that both, cortical areas and input projections from thalamic neurons, express Cdh6 or Cdh8, suggesting that Cdhs could comprise a molecular code for wiring (Suzuki et al., 1997). Likewise, mossy fibers (MF) and their CA3 targets in the hippocampus were positive for Cdh9. Absence of Cdh9 in either MF or CA3 neurons selectively reduces their synaptic connectivity (Williams et al., 2011). Both scenarios suggest that Cdhs wire these populations together.

1.6.3 Instructive role of Cdh in lamina assignment

Cdhs play a central role in the assignment of neurites to appropriate IPL sublaminae in the mouse retina. Recent work in DS circuits (see 1.4.2 above) showed that selective expression of Cdhs instruct BC and DSGC processes towards a specific sublamina. DS circuits contain Cdh8+ OFF-BC2s that project their axons into S2, and Cdh9+ ON-BC5s that grow axons into S4; the postsynaptic DSGC and AC partners of these BCs reside in these sublaminae (Duan et al., 2014). In double *Cdh8* and *Cdh9* knockouts axons of OFF-BC2s and ON-BC5s randomly project to both S2 and S4. This Cdh depletion also resulted in a severe disruption of OFF or ON DSGC responses but did not affect the sublayer position of DSGCs or SACs (Duan et al., 2014). Subsequently, another study showed that Cdh6, 9, and 10 are expressed in DSGCs and SACs. They generated triple *Cdh6*, *9*, and *10*

mutants and saw that dendrites of ventral DSGCs (vDSGCs), but not SACs, disseminate out of s2 and s4 (Duan et al., 2018). To test if SACs serve as a scaffold for BCs and vDSGCs, SACs were ablated which resulted in a similar phenotype as triple *Cdh6*, *9*, and *10* knockouts. Altogether suggests that in the DS circuit, Cdh8 and 9 force BCs to choose between S2 and S4; Cdh6, 9, and 10 guide vDSGCs into s2 and s4; and BCs and vDSGCS use SACs as a scaffold to organize their processes.

Interestingly, sequencing studies revealed that Cdh7 is expressed in nasal motion selective DSGCs (nDSGCs) and its binding partner Cdh18 in SACs. When Cdh7 is disrupted nDSGCs dendrites diffuse out of S2 and S4 but SAC dendrites position remain unaltered, resembling the triple *Cdh6*, *9* and *10* knockout phenotype (Duan et al., 2018). This further supports the idea that SACs express Cdhs to scaffold projections from later-born neurons. Taken together, these results suggest that Cdh expression among DSGCs, BCs, and SACs directs these cells to a common pair of layers and creates direction selective circuitry.

The idea of an existing scaffold that retinal neurons can use to organize their processes offers the advantage of robustness. A Cdh can guide a developing neuron into a sublamina and be reused to recruit subsequent laminating partners. scRNA-seq studies could help to unveil if spatiotemporal Cdh-expression pattern like this exists to wire neuronal circuits in an organized manner.

2. Hypothesis and specific aims

Cumulative evidence suggests that members of the Cdh superfamily play a role in targeting retinal neurons into a specific sublamina of the IPL (Duan et al., 2014, 2018). Yet, we still lack a

study showing if Cdhs expression patterns change across multiple retinal types and if this expression is conserved from a developing to a mature retina. The hypothesis of this project postulates that a stereotyped set of Cdhs will be expressed by retinal types to guide them into one of the 5-10 possible IPL sublaminae. To test this idea, the aims of this thesis are:

1) To define the Cdh expression patterns in retina across retinal cell subtypes.
2) To compare expression of Cdhs in the developing and mature retina.
3) To postulate Cdh candidates that might mediate IPL sublaminar choices.

3. Methods

3.1 Animals

Cdh4 CreER mice were generated by targeted insertion of a FRT flanked neo cassette, a 6xmyc-tagged CreER-T2, and a poly-adenylation signal replacing the N-term 19 amino acid at the translational start site of the *Cdh4* coding sequence via homologous recombination in embryonic stem cells as described previously for *Cdh6 CreER* mice (Kay et al., 2011). The targeting vector was generated by lambda phage-mediated recombineering (Chan et al., 2007). This removed the N-terminal 19 amino acids (MTTGSVLPLLLLGLSGALR) of Cadherin 4 protein. Chimeric mice with the targeted embryonic stem cells were generated and mated to obtain germ line transmission by the Harvard University Genome Modification Facility. *Cdh4 CreER* mice were crossed with reporter mice containing a lox-stop-lox-YFP cassette (Buffelli et al., 2003) and a Cre-dependent GCaMP6f (Fig. 3) (Chen et al., 2013). Tamoxifen (2 mg to 8 mg, Sigma) was injected intraperitoneally into double transgenic mice, either neonatally or in adults, to label cells. All mice

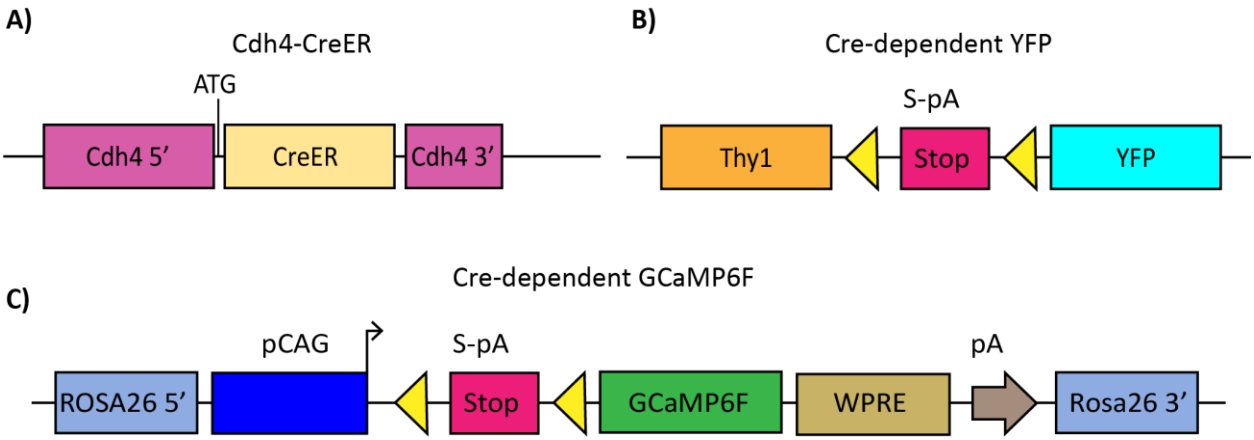

Figure 3. Mouse lines. A: knock-in/knock-out tamoxifen-inducible Cre/ERT2 from the mouse *Cdh4* promoter. **B**: Reporter yellow fluorescent protein (YFP) gene under the control of the neuron-specific regulatory elements from thy1 gene. Stop sequence is Cre-dependent removed. **C**: Fluorescent calcium-indicator (GCaMP6f) coupled with the expression enhancer WPRE, and under the synthetic promoter pCAG. This gene inserted in the ROSA locus is used to detect neuronal responses when the Cre-dependent STOP sequence is removed.

were maintained on a C57BL6 background. These procedures were performed in accordance with the Canadian Council on Animal Care (CCAC).

3.2 Immunohistochemistry

Young adult mice (1-3 months old) were euthanized by isoflurane overdose and perfused with room-temperature phosphate buffered saline (PBS) followed by chilled 4% paraformaldehyde (PFA) in PBS. Eyes were removed and post-fixed in 4% PFA at 4°C for 1 hour and retinal tissue was dissected.

3.2.1 Cross-sections

For analysis of sections, retinas were postfixed for 1 h, incubated with 40% sucrose/PBS overnight, frozen, and sectioned at 30 µm in a cryostat. Sections were incubated with 10% blocking buffer (10% donkey serum/0.4% Triton X-100/PBS) for 2 h, and 4% blocking buffer (4% donkey serum/0.4% Triton X-100/PBS) with primary antibodies overnight at 4°C, and with

secondary antibodies for 2 h at room temperature. In some cases, DAPI (NucBlue, ThermoFisher Scientific) was included after secondary antibodies as a nuclear staining. Sections were cover-slipped with Fluoromount™ Aqueous Mounting Medium (Sigma-Aldrich).

3.2.2 Wholemounts

For whole mounted retinas, primary antibodies were incubated in a 4% blocking buffer at 4°C for a week and secondary antibodies at 4°C overnight. Tissue was then flat-mounted on membrane filters, and cover-slipped with Fluoromount™ Aqueous Mounting Medium (Sigma-Aldrich).

3.2.3 Antibodies

Primary antibodies used in this study are as follows: chicken anti-GFP (Abcam ab13970), goat anti-Osteopontin (R&D Systems AF808), mouse anti-Ap2α (DHSB AB_528084), goat anti-vAChT (Millipore Sigma ABN100). Secondary antibodies were Fluorescein (Millipore AP180F); Alexa Fluor 647 (Millipore AP180SA6, AP192SA); Cy3 (Millipore AP180C, AP182C); Alexa Fluor 488 (Cedarlane 703-545-155); Alexa 405 (Abcam ab175649).

3.3 Tamoxifen injections

Tamoxifen (Sigma) was dissolved in sterile sunflower oil (Sigma) by sonication and intraperitoneally administered at 50 ug/g animal. After two weeks animals were euthanized, and retinal tissue was dissected.

3.4 Expression Analysis

For expression analysis scRNA-seq data organized in clusters from pups (Rheaume et al., 2018) and adults (Tran et al., 2019) mice was retrieved from NCBI GEO (accession number GSE115404

and GSE133382, respectively). Pups were clustered in 41 groups while adult data contained 45 groups. Subsequently, data was processed using R 3.5.3.

To match subtypes across clusters from pups and adults I used the top marker combinations described in Tran et al., 2020 that define adult RGC clusters. These markers are combinations of one to three genes that are uniquely depleted or enriched for a specific cluster with at least one of them enriched. I calculated the percentage of cells satisfying these expression patterns and the average transcript count of enriched markers per cluster, using expression data for pups and adults. The average expression of a marker combination was normalized to 1 across pup clusters and across adult clusters. Next, I used expression levels from Rheaume et al., to find the pup RGC cluster whose expression most closely mimicked the adult RGC marker combinations over the other pup clusters and matched with the corresponding adult RGC subtype. If a pup RGC cluster did not meet this criterion, then it was assigned an adult RGC subtype based on the highest expressing markers combination within the pup cluster.

4. Results

4.1 Single-cell RNA-seq analysis of RGC subtypes

Recent evidence suggests that Type II Cdhs may act as sublaminar targeting cues (Duan et al., 2014, 2018). To learn more, I asked whether RGC subtypes defined by gene signatures express different Cdh members during IPL lamination. To test this idea, I looked at the expression of specific RGC subtypes markers and Cdh expression patterns in each RGC subtype at two developmental timepoints.

4.1.1 Combinatorial markers that define adult RGC subtypes are already expressed at P5

RGC subtypes present different expression profiles and project to different sublayers of the IPL (Rousso et al., 2016; Basu et al., 2017; Duan et al., 2018; Laboissonniere et al., 2019; Tran et al., 2019; Nguyen-Ba-Charvet and Rebsam, 2020). Two recent scRNA-seq studies that target P5 and adult RGCs offer an ideal dataset to correlate Cdh expression to sublaminar selection. Each study defined RGCs according to gene expression but only the adult dataset contained annotation relating these molecular definitions to existing RGC types. Annotating the P5 dataset with current RGC type definitions is critical to link the newborn RGCs in this dataset with their adult counterparts, and to their sublaminar targeting patterns. To do this, I searched for markers of adult RGC subtypes in the P5 dataset. Adult data was retrieved from Tran et al., 2019, who grouped RGCs into 45 clusters (A1-A45) according to a unique combination of expressed genes. P5 data as retrieved from Rheaume at al., which defines 40 RGC clusters (PP1-PP40) according to similar methods.

To relate these datasets, I asked if adult RGC clusters definitions could be used to identify their younger counterparts. If true, then the RGC-type annotation from the adult dataset could be propagated backwards to the P5 data. I discovered that marker combinations used to define adult RGCs could, in many cases, be used to define clusters in pups (Fig. 4A). In many cases, the expression of other genes in each adult cluster corresponded with its P5 counterpart. Given the differences in cluster number in these studies, some clusters in pups correspond to more of one RGC subtypes (e.g. PP9) or many clusters to more than one subtype (e.g. PP22 and PP23 labelled as ooDS DV). This could represent the presence of intermediate subpopulations during differentiation or differences in clustering methods giving that the subtypes in the same cluster

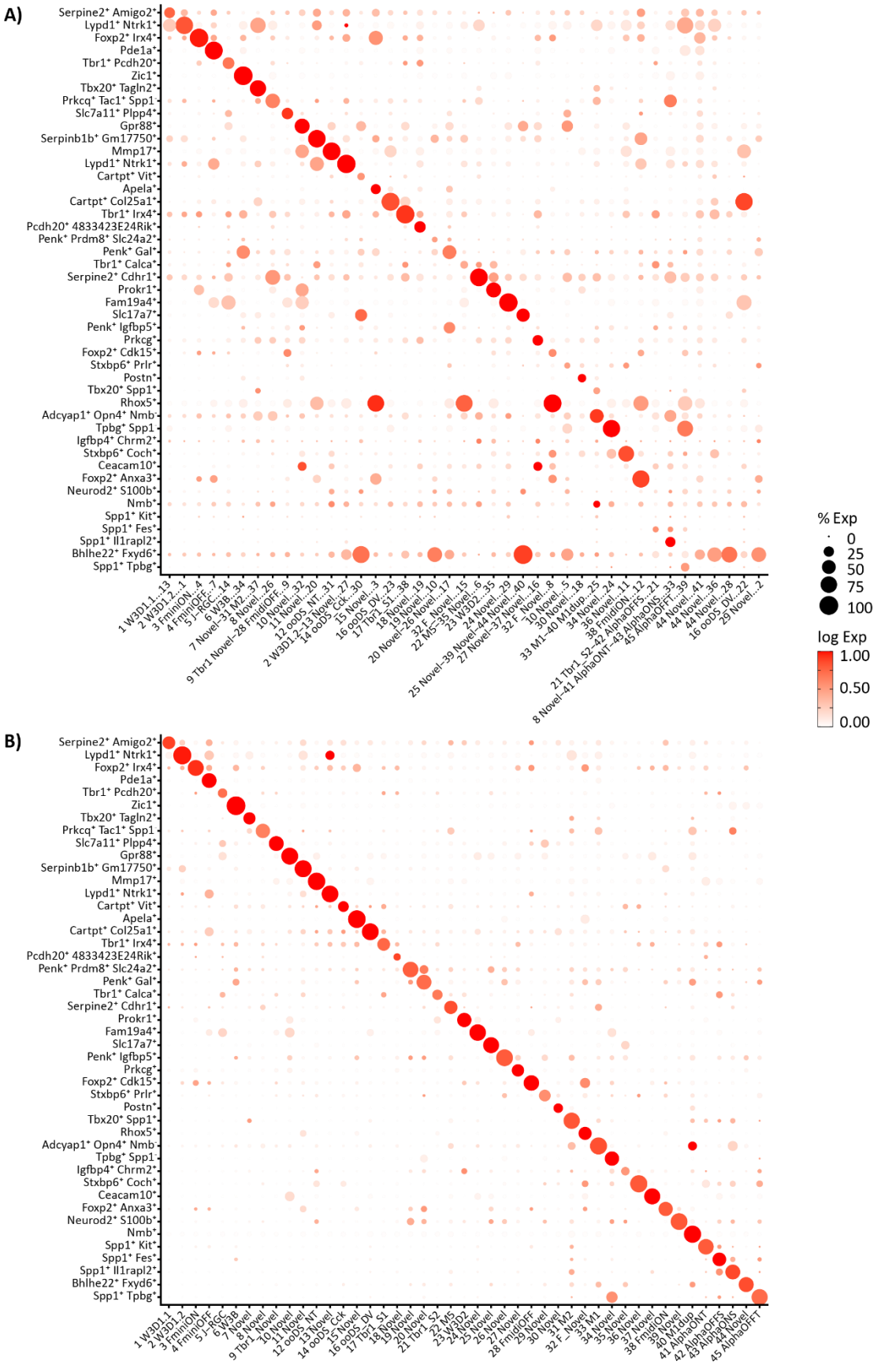
A)
B)
% Exp
0
25
50
75
100
log Exp
1.00
0.50
0.00

Figure 4. scRNA-seq analysis shows that many molecularly defined RGC subtypes in adult mice are already present at P5. A: Expression of specific adult RGC subtype markers in P5 mice clusters. Pup clusters were named based on the most expressed marker combinations across and within cluster. **B**: Adult RGC subtype expression of marker combinations reproduced from Tran et al. (2019). Dotplots display makers combinations in the y axis and RGC subtypes in the x axis. Marker combinations are composed enriched (+) and depleted (-) genes. The size of the circle represents the percentage of cells within the cluster that satisfied the combination pattern, and the color the cluster average expression of enriched genes normalized to 1 across clusters.

are not closely related (e.g. PP33 as Tbr1 S2 and Alpha OFFS). Despite these differences, most of the clusters show strong correspondence between P5 and adult clusters, allowing us to label P5 clusters as known RGC types (Fig. 4). Armed with this definition, I next investigated the pattern of Cdh expression across RGCs.

4.1.2 Patterns of Cdh expression across RGCs subtypes vary

To assess Cdh expression pattern across RGC subtypes, I generated cell type specific Cdh expression maps of RGCs in both the P5 and adult datasets (Fig. 5). As expected, distinct members of classical Cdhs were expressed in different patterns by RGCs. *Cdh4* in W3D2 (S3), J-RGCs (S1) and alpha-OFF-T (S3); *Cdh6* in OODS DV (S2,S4); *Cdh11* in OODS Cck and OODS NT (S2, S4); *Cdh13* W3B (S3), W3D1 (S3) and F-miniON (S3) (Fig. 6) (Kim et al., 2008; Krishnaswamy et al., 2015; Rousso et al., 2016; Krieger et al., 2017; Duan et al., 2018); and other Cdhs in many other novel groups (Fig. 5). Cdh expression patterns appear conserved between P5 (Fig. 5A) and adults (Fig. 5B) consistent with the idea that Cdhs define sublaminar locations for developing RGCs and enforce sublaminar choice during adulthood. Moreover, the exclusive pattern of Cdh expression across RGC types targeting different sublaminae supports the hypothesis that Cdh isoforms encode IPL position.

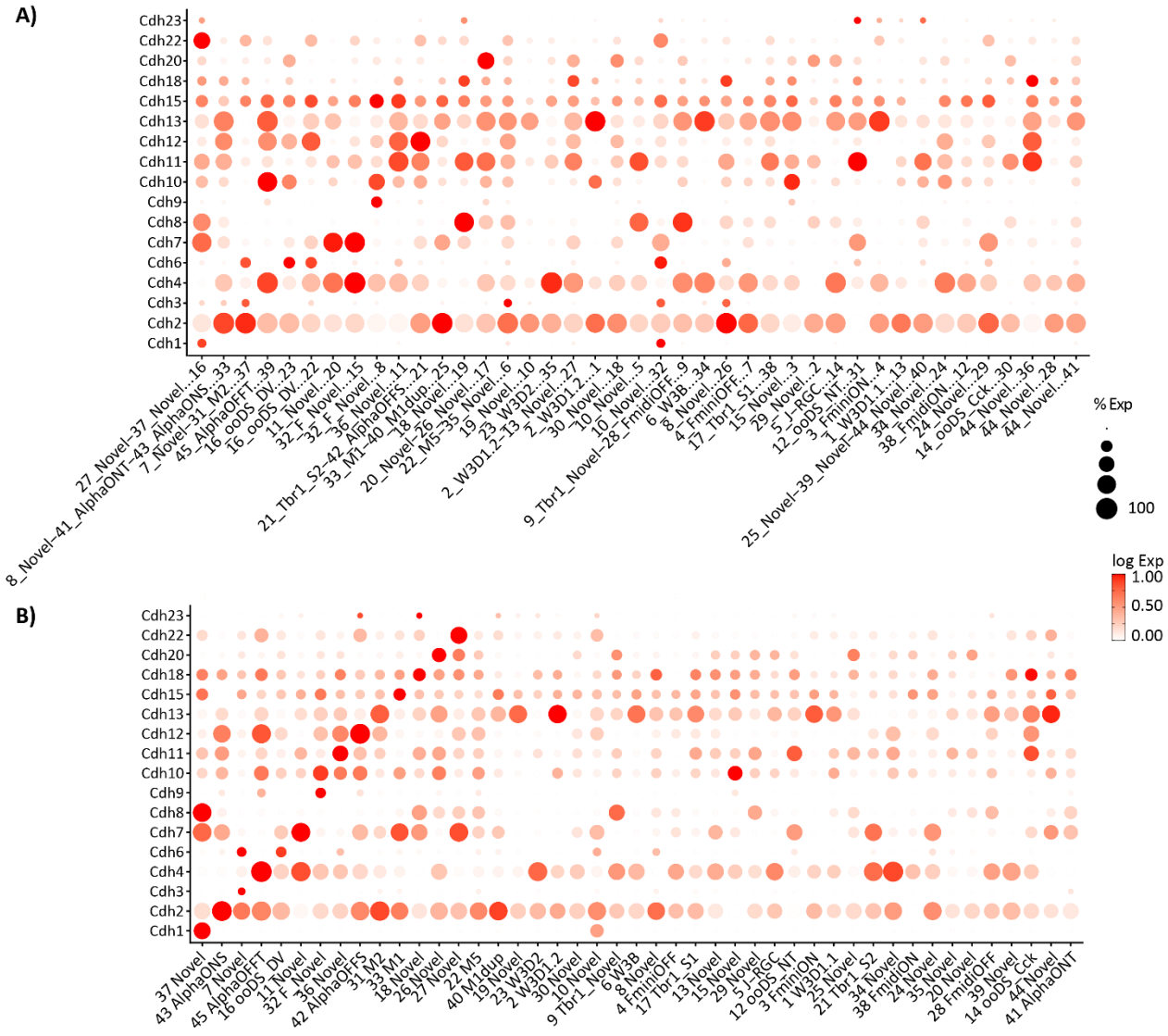

Figure 5. scRNA-seq analysis of classical Cadherins reveals their expression in distinct patterns across RGC subtypes. A: Cdh expression at P5 mice. **B**: Cdh expression in adult mice. Dotplots display Cdhs in the y axis and RGC subtypes in the x axis. The size of the circle represents the percentage of cells within the cluster that express a specific Cdh, and the color the cluster average expression that Cdh normalized to 1 across clusters.

Figure 6. Cadherin expression patterns are conserved from P5 to adults in RGC subtypes. Comparison of Cdh expression across previously defined RGC subtypes shows the similarity in expression patters among P5 (blue) and adult (red) retinas. Dotplots display Cdhs in the y axis and RGC subtypes in the x axis. The size of the circle represents the percentage of cells within the cluster that express a specific Cdh, and the color the cluster average expression that Cdh normalized to 1 across clusters.

4.1.3 *Cdh4* is highly expressed in specific RGC subtypes

From this analysis, I focused on *Cdh4*. This Cdh was first described in the developing retina in chickens and named R-Cadherin due to its high expression in this tissue (Inuzuka et al., 1991). Later, Babb et al. described a loss of discrete laminae in *Cdh4* mutant in fish (Babb et al., 2005). In mouse, Cdh4 expression has been reported in some RGCs subtypes (Rousso et al., 2016; Liu et

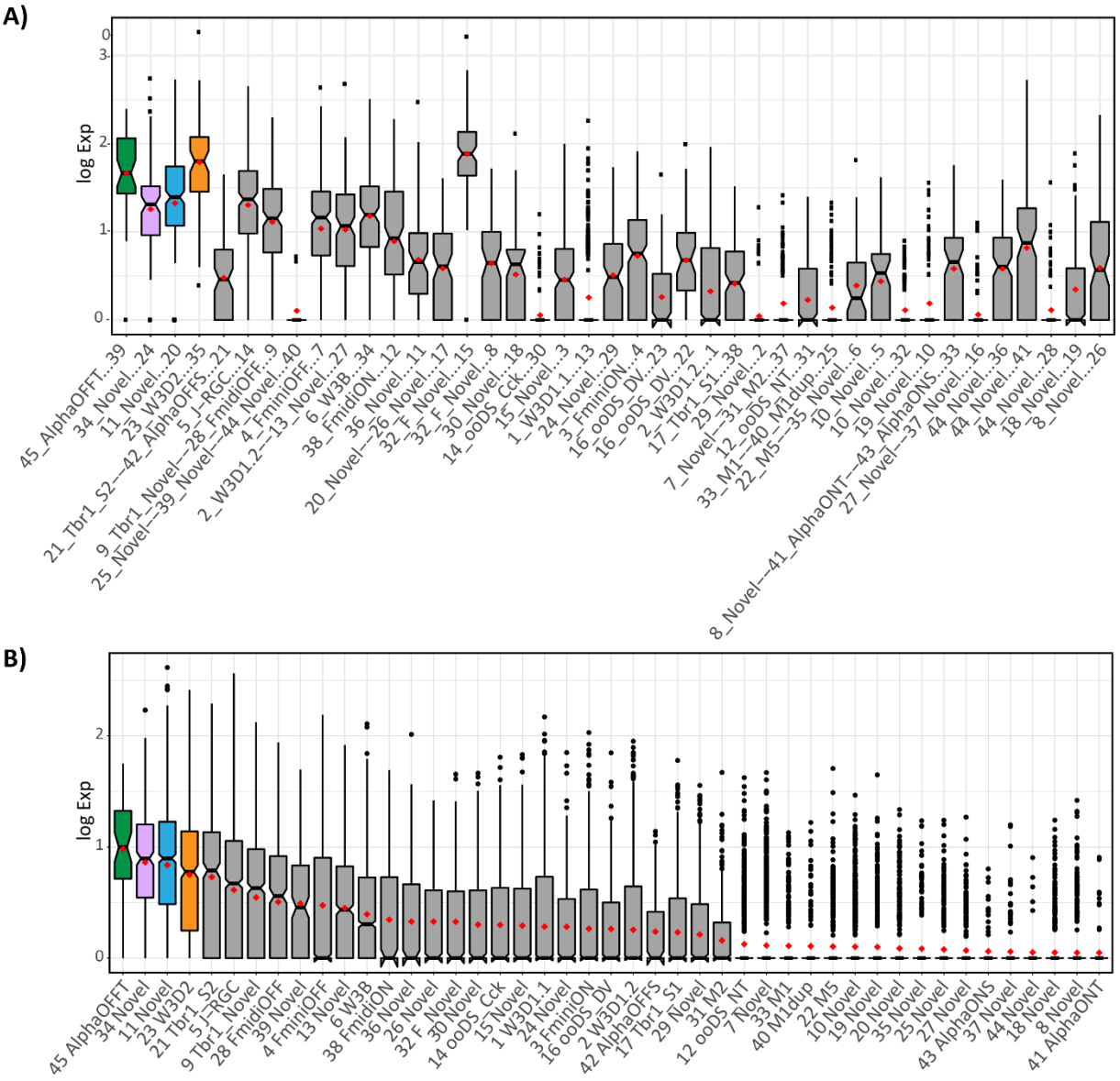

Figure 7. *Cdh4* is highly expressed in the same specific subtypes across development. A: *Cdh4* expression in P5. The number after '..' indicates the corresponding cluster number in Rheaume et al. (2018). PP39 (green), 24 (pink), 20 (blue) and 35 (orange) clusters are highly expressed as in adults. **B**: *Cdh4* expression in adult mice. Boxplots show *Cdh4* expression across RGC subtypes ordered from higher to lower expression in adults (left to right). Black dots represent outliers and red dots the mean expression for each cluster.

al., 2018). However, the role of Cdh4 in the vertebrate retina is still unknown. To learn more, I analyzed its expression in my RGC expression data and found that it labels the same RGC types in the P5 and adult datasets (Fig. 7). These types correspond to RGCs that limit their projections

to the upper half of the IPL. Together, this result suggests that these neurons use Cdh4 to target the upper IPL laminae.

4.2 Molecular description of Cdh4 cells in the retina

4.2.1 *Cdh4* mouse lines

For further characterization of Cdh4+ cells, I used a mouse line in which *Cdh4* gene was disrupted by insertion of a Cre-ER transgene ($Cdh4^{CreER}$) (Fig. 3A). As heterozygotes ($Cdh4^{CreER/+}$), this line allows to mark and manipulate Cdh4+ve neurons, as homozygotes they are *Cdh4* knockouts ($Cdh4^{CreER/CreER}$). I mediated Cdh4+ve cells labelling by crossing three generation of *Cdh4* mice with two Cre-dependent reporter lines: 1) a Cre-dependent *YFP* (*THSTP15*) (Fig. 3B) (Porrero et al., 2010) and 2) a Cre-dependent calcium indicator GCaMPG6f (G6f) (Fig. 3C) (Chen et al., 2013). *THSTP15* is under *thy1* promotor which transcribes a surface glycoprotein highly expressed in RGCs (Barnstable and Dräger, 1984) and with weak expression in cholinergic amacrine cells (Raymond et al., 2008), thus, I used it to study Cdh4+ve RGCs (C4RGCs) morphology. G6f is under the synthetic CAG promoter, a constitutive promoter in mammals that drives high expression regardless of cell type, allowing a more comprehensive characterization of Cdh4+ve retinal types. *Cdh4* heterozygotes were used in the next experiments to identify Cdh4+ve retinal cell types and homozygotes will be used for further directions of this project to study mutant phenotypes.

4.2.2 Cdh4 labels RGCs, ACs and HCs

I obtained retina cross-sections of $Cdh4^{CreER/+}G6f$ mice injected with tamoxifen at P14 and adult (>P45) to characterize Cdh4+ve cells; mice open their eyes between P12-14. Reporter labelling was found in the GCL, the lower INL, and upper INL, suggesting that ACs, HCs, and RGCs may

express Cdh4 (Fig. 8A). Immunostaining these sections with the AC-specific marker AP2α revealed overlap with reporter positive cells in the INL but not the GCL, indicating that Cdh4 is expressed in RGCs and ACs (Fig. 8B). Three retinal types were found to be label as Cdh4+ve. First, cells localize next to the apical section of the INL stratifying into the OPL were classified as HCs (Fig. 8A, yellow arrow). Second, neurons in the basal region of the INL and in the GCL stratifying into the IPL positive for AP2α were determined to be ACs (Fig. 8B, yellow arrow) (C4-ACs). Third, AP2α negative cells in the GCL with dendrites in the IPL were identified as RGCs (C4RGCs) (Fig. 8B, cyan arrow). These patterns of expression are conserved in retinas from P14 and adults and no reporter labelling were found in the ONL nor were the reporter labelled cells in the INL with a BC morphology. Thus, Cdh4 labels a subset of ACs and RGCs from the period of IPL genesis into adulthood.

4.2.3 AC and RGC Cdh4+ve project to S1-S3 of the IPL

If Cdh4 plays a role in targeting the dendrites of developing C4RGCs and C4-ACs then these neurons should inhabit a common IPL location in adults. To test this idea, I analyzed the morphology of Cdh4+ve neurons in retinal cross-sections from *Cdh4*$^{CreER/+}$*G6f* retinas. Sublaminae were identified using antibodies to vAChT which label dendrites in S2 and S4. I observed that C4-AC and C4RGC processes densely innervate S1 to uS3 of the IPL (Fig. 8C). This agrees with the

scRNA-seq data in which *Cdh4* had the highest expression neurons that were previously described to project to upper layers: W3D2 (S3), J-RGCs (S1) and alpha-OFF-T (S3).

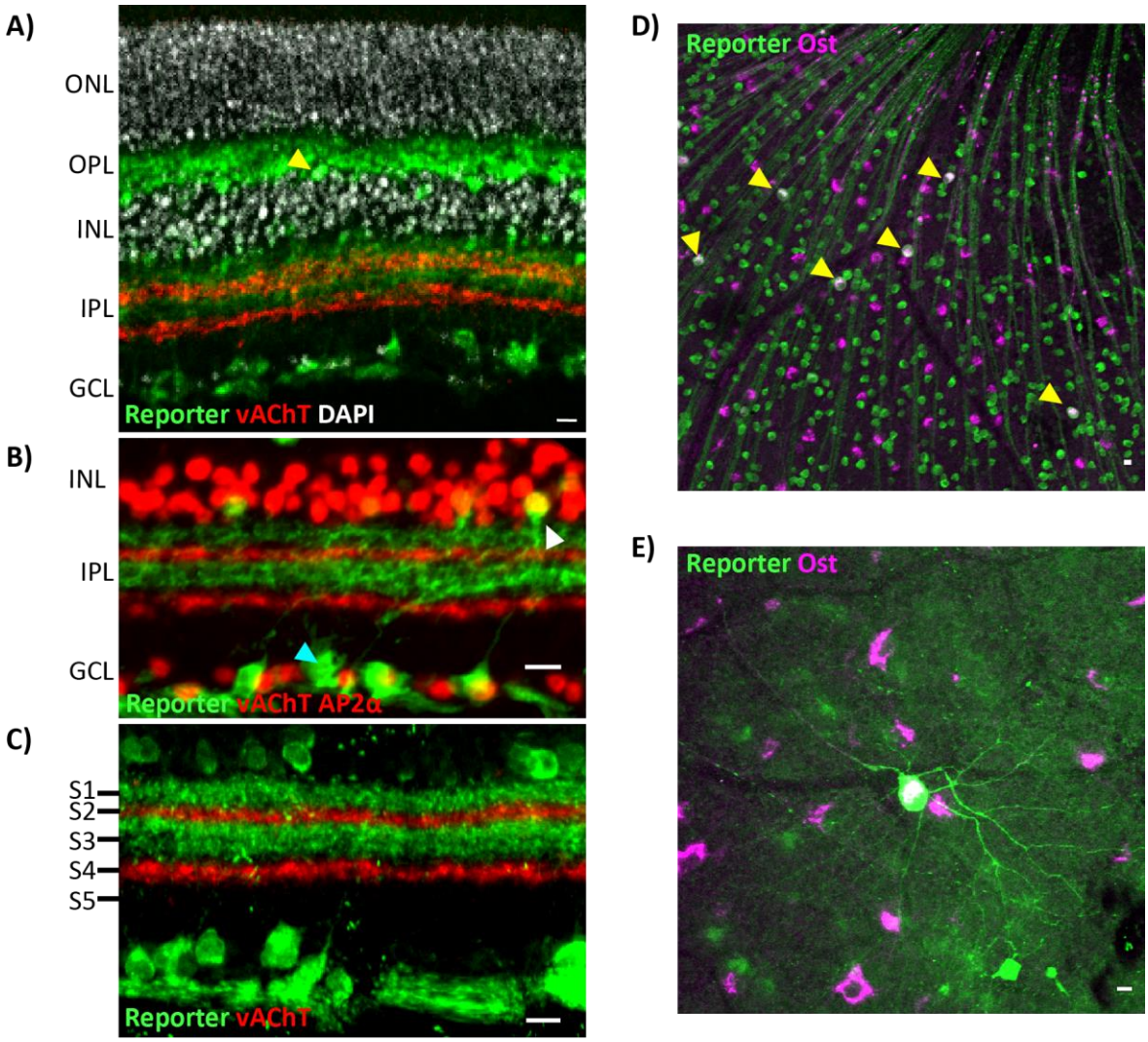

Figure 8. C4-ACs and C4RGC project from S1 to upper S3 of the IPL. A: Retina cross-section showing the expression of the Cdh4 reporter restricted to the INL, IPL and GCL. Yellow arrow point to a Cdh4+ve HC. **B**: Retina cross-section showing the expression of Cdh4 reporter in ACs and RGCs. White arrow points to a Cdh4+ve cell co-expressing the AC marker AP2α (C4-AC) and cyan arrow to a Cdh4+ve cell negative for AP2α in the GCL (C4RGC). **C**: Retina cross-section showing that C4-AC and C4RGC projections only populate from S1 to upper S3 of the IPL. **D**: Whole mount retina immunostaining for Cdh4 reporter combined with antibodies against Osteopontin (Ost), an αRGC marker. Yellow arrows point to RGCs co-expressing the Cdh4 reporter and Ost (Cdh4+ve αRGCs). **E**: Morphology of a Cdh4+ve αRGCs cell identified with the Cdh4 reporter and Ost. vAChT labels S2 and S4 (A-C). Scale bars represent 10 µm.

4.2.4 C4RGC population contains αRGCs

To validate expression data and relate it to the possible role of Cdh4 in IPL lamination I started by validating the RGCs subtypes predicted to express *Cdh4* in my scRNA-seq analysis. One of these subtypes was an αRGC, therefore, I stained whole *Cdh4*$^{CreER/+}$*G6f* retinas for Osteopontin, a protein known to be expressed only in αRGCs (Krieger et al., 2017). As predicted, I observed co-localization of the C4RGC marker, G6f, and Osteopontin (Fig. 8D and E, yellow arrows). Thus, C4RGC population contain αRGC and, as indicated by RNA-seq, this could be a αRGC transient.

5. Discussion and contributions to original knowledge

The retina is a well-organized structure where processes of more than 100 retinal neuron subtypes are confined in the IPL during development. Here, neurons synapse selectively with one another to create feature detecting circuits. How this synapse specificity is achieved is not altogether clear. One hypothesis is that processes are organized into sublaminae to diminish the number of available potential partners and thus, reduce complexity. Cdhs have been postulated as the recognition molecules that guide this lamination in the IPL. If true, some conditions need to be fulfilled: 1) the existence of neuron subpopulations during IPL development so each follow their own cues to a specific sublamina; 2) Cdh expression patterns defining each of these subpopulations; and 3) cells expressing the same Cdh laminate to the same region of the IPL. In this thesis I provide evidence that indicates these conditions are true for Cdh expression and I started the characterization of Cdh4 to better understand its role in retinal circuit assembly.

5.1 Elucidating Cdh role in the retina

For Cdhs to guide neuron processes they must be part of the set of genes that define specific genetic cell profiles during development, and therefore, be expressed in different patterns across retinal neuron subtypes. My expression analysis in classical Cdhs shows that: 1) Cdhs are part of the genes that change expression levels across RGC subtypes; 2) different subtypes have a specific Cdh expression pattern; and 3) Cdh expression patterns are conserved across development from P5 to adult retinas. Thus, I provide support to the hypothesis of Cdhs as the molecular signals that guide neurons.

RGCs project their neuronal processes to one or two specific IPL sublamina as they differentiate into subtypes. The presence of the molecules responsible to guide these processes is therefore needed at this stage of retina development. My results show that multiple Cdh isoforms are expressed across RGC subtypes at P5, when RGCs undergo differentiation and retina circuits are assembled. Each RGC subtype present a different expression pattern of Cdhs. Within these expression patterns, one or a few Cdhs are highly expressed and RGCs subtypes that project to the same IPL sublamina show high expression of the same Cdh isoform. Whether one or more than one Cdh is needed by a single RGC subtype to locate their processes is not completely clear. There is evidence in BCs that shows how mutations in a single Cdh can drive IPL miss targeting (Duan et al., 2014) while in ooDSGCs the expression of different Cdh isoforms results in a compensation mechanism when one Cdh is mutated (Duan et al., 2018). Taken together, my results support the idea that Cdhs guide specific RGC subtype adhesion during retina development but to better understand the role of Cdhs in neuronal circuit assembly, it is necessary to study how they are orchestrated together during development.

Classical Cdhs are found in the developing and adult CNS with complex and dynamic expression patterns (Suzuki et al., 1991, 1997; Redies, 2000). In this thesis, I studied the expression patterns of Cdhs in pups and adult retinas to test if they change across development. I analyzed scRNA-seq data of P5 and adults RGCs and showed that Cdh expression patterns present during RGC differentiation are conserved in the fully developed eye. RGC subtypes that have been previously studied individually and confirmed as pure subtypes showed a clear similarity at P5 and adulthood. Yet, some subtle differences in Cdh expression are observed. This could be due to refinement of Cdhs expression as the eye finishes its development or result of cross-contamination of RGC subtypes within our clusters. To further understand these differences, individual RGC subtypes need to be studied. Overall, my results agree with the idea that Cdhs define the location of dendrites and axons into the IPL for developing RGCs and reinforce these choices during adulthood to maintain circuit organization.

Cdh4 is also known as retina Cdh because it was characterized for the first time in the retina (Inuzuka et al., 1991). Yet, its role in the retina is unknown. I started Cdh4 characterization in the mouse retina to test if it has a role in circuit assembly, with special focus in lamination. Using scRNA-seq data I found that high expression levels of *Cdh4* are restricted to a subset of RGC subtypes; some of them have been previously studied and show that their processes range from S1 to S3 (Kim et al., 2008; Krieger et al., 2017). Additionally, I generated a mouse line in which the *Cdh4* gene was interrupted by CreER and in concert with Cre-dependent reporters, I show that Cdh4 is restricted to a few retinal neurons: HCs, ACs and RGCs. Within this cell population, in retina cross-sections, I found that C4RGC and C4-AC projections are restricted to the upper part of the IPL as predicted by my expression analysis of Cdh4. This suggests that Cdh4 restrict

lamination towards the OFF region of the IPL which has been previously defined to go from S1 to uS3 (Chalupa and Günhan, 2004). Lastly, as predicted by my RNA-seq analysis, I confirmed the presence of αRGCs in the Cdh4 neuron population by immunostaining against Osteopontin, a marker that specifically labels αRGCs. This and further characterization of Cdh4+ve neuron subtypes will allow us to investigate the role of Cdh4 by genetically manipulating specific subtypes to study their individual lamination and functional phenotypes when Cdh4 is deleted.

5.2 Adhesive code model

To better understand wiring specificity, as Cdh function starts to be elucidated it needs to be brought into the context of other molecules that also mediate circuit assembly. Many studies have identified some of these molecules and their functions. As result, the idea of an adhesive code is emerging.

Recent studies propose that already laminated neurons might form a scaffold that later other neurons use when laminating. This evidence comes from SACs; they are one of the first neurons that project into the IPL and they do so using Megf10, who was described to diffuse SAC projections into S2 and S4 (Ray et al., 2018). Another study showed that SACs and their synaptic partners, vDSGCs, express Cdh6, 9 and 10, and triple knockdowns of these Cdhs only affect arbor positioning of vDSGCs but not SACs (Duan et al., 2018). Putting together these results suggest that while molecules like Megf10 mediate the assembly of a scaffold of first-born neurons, subsequent developing neurons, like vDSGCs, laminate towards this scaffold using Cdhs.

Beside attractive proteins, other molecules have been shown to mediate repulsion signals during retina development, like Semas and their Plex receptors. Sema5A and 5B and their Plex

receptors led to the separation of nuclear layers from plexiform layers (Sun et al., 2013). Additionally, recent studies show that Semas also play a role in segregating ON and OFF neurons. Sema6A labels the dendrites of ON types, whereas PlexinA4 and PlexinA2 are expressed in OFF types causing ON and OFF cells to repulse each other (Sun et al., 2013). My results showing that Cdh4+ve neurons project only to the OFF region of the IPL open the possibility that an interplay of repulsive and attractive signals, from Sema6A/PlexA4-A2 and Cdh4 respectively, mediate the physical separation of ON and OFF circuits.

Finally, laminae simplify wiring complexity because they bring into close proximity neuron partners and place inappropriate ones far apart (Sanes and Yamagata, 2009; Baier, 2013). But even then, later-born neurons must find their partners in an overcrowded space. So it has been postulated that once Cdhs guide neuron processes into the right layer, the immunoglobulin (Ig) superfamily comes into play to help neurons choose specific partners (Krishnaswamy et al., 2015; Tan et al., 2015; Xu et al., 2018). In the mouse retina, the Ig member Sidekick 2 (Sdk2) was implicated in enrich connections among co-laminar ACs and RGCs (Krishnaswamy et al., 2015). The activation of Sdk2+ve VG3-ACs, which dendrites reside in S3, resulted in higher activation of close Sdk2+ve W3B-RGCs than equally approximated Sdkv2-ve RGCs. Sdk2 disruption caused connectivity loss and reduce strength of the remaining connections among VG3-ACs and W3B-RGCs. Thus, expression of a unique combination of recognition molecules from the Cdh and Ig superfamilies might direct neuronal processes to specific neuropil layers and specific synaptic targets, respectively. This implies that Ig could be reused in different layers if a different Cdh is expressed.

5.3 Future directions

The generalizability of my expression pattern results is limited to RGCs by the scRNA-seq data available. New AC and BC published data (Yan et al., 2020) will allow me to expand my findings in Cdh expression to these other neuron types and help to predict which AC subtypes express *Cdh4*. Additionally, my preliminary results in Cdh4 provide insights of its role as a mediator in OFF and ON channel segregation. However, proving that lamination disruption is a *Cdh4* mutant phenotype will be key to fully link Cdh4 with ON and OFF neuron segregation. Furthermore, it needs to be functionally tested that in fact Cdh4+ve cells in their majority evoke OFF responses. If true, it will be interesting to investigate the existence of a functional shift from OFF to ON responses that might result from misslamination in *Cdh4* mutants. To perform these future experiments, in this thesis project I have prepared *Cdh4*$^{+/CreER}$*G6f* mouse lines to record Cdh4+ve neurons responses and test if their OFF anatomical position of their processes agrees with functionality. In addition, I bred *Cdh4*$^{CreER/CreER}$*G6f* mice to look at IPL projections of Cdh4+ve mutant neurons and consequences in functional responses. Given that G6f is a fluorescent calcium indicator, neurons responses can be easily recorded using two photon calcium imaging (Euler et al., 2009; Baden et al., 2016). These mouse lines can also be coupled with mapping methods, like Cre-dependent rabies tracing, to map interneuron synaptic partners of C4RGCs (Yonehara et al., 2011; Dhande et al., 2013). Lastly, as these studies evolve, it will be of interest to missexpress Cdh4 in normally Cdh4-ve RGCs in the ON region of the IPL and ask if their dendrites can be biased to S1-uS3 to prove causality of Cdh4 in guiding processes into the OFF region.

6. Conclusion

My work joins the effort to begin to unearth rules and blueprints that wire the retina. In this thesis I provide evidence to support the hypothesis of Cdhs as the adhesion molecules that guide neuron processes to the right sublamina, and the first insights that Cdh4 might play a role in segregating ON and OFF processes in the IPL. These results and other recent studies outline an adhesion code compose of attractive and repulsive signals to assembly retina circuits. Learning more about Cdhs and other adhesion molecules in the retina circuits will keep building upon the adhesion code model to peer into the wiring problem into the brain.

7. References

Ahnelt, P. K., and Kolb, H. (2000). The mammalian photoreceptor mosaic-adaptive design. *Progress in Retinal and Eye Research* 19, 711–777. doi:10.1016/S1350-9462(00)00012-4.

Amini, R., Rocha-Martins, M., and Norden, C. (2018). Neuronal Migration and Lamination in the Vertebrate Retina. *Front Neurosci* 11. doi:10.3389/fnins.2017.00742.

Applebury, M. L., Antoch, M. P., Baxter, L. C., Chun, L. L. Y., Falk, J. D., Farhangfar, F., et al. (2000). The Murine Cone Photoreceptor: A Single Cone Type Expresses Both S and M Opsins with Retinal Spatial Patterning. *Neuron* 27, 513–523. doi:10.1016/S0896-6273(00)00062-3.

Baccus, S. A., Ölveczky, B. P., Manu, M., and Meister, M. (2008). A Retinal Circuit That Computes Object Motion. *J. Neurosci.* 28, 6807–6817. doi:10.1523/JNEUROSCI.4206-07.2008.

Baden, T., Berens, P., Franke, K., Rosón, M. R., Bethge, M., and Euler, T. (2016). The functional diversity of retinal ganglion cells in the mouse. *Nature* 529, 345–350. doi:10.1038/nature16468.

Baier, H. (2013). Synaptic laminae in the visual system: molecular mechanisms forming layers of perception. *Annu Rev Cell Dev Biol* 29, 385–416. doi:10.1146/annurev-cellbio-101011-155748.

Ballesta, J., Terenghi, G., Thibault, J., and Polak, J. M. (1984). Putative dopamine-containing cells in the retina of seven species demonstrated by tyrosine hydroxylase immunocytochemistry. *Neuroscience* 12, 1147–1156. doi:10.1016/0306-4522(84)90009-5.

Barlow, H. B., and Levick, W. R. (1965). The mechanism of directionally selective units in rabbit's retina. *The Journal of Physiology* 178, 477–504. doi:10.1113/jphysiol.1965.sp007638.

Barnstable, C. J., and Dräger, U. C. (1984). Thy-1 antigen: A ganglion cell specific marker in rodent retina. *Neuroscience* 11, 847–855. doi:10.1016/0306-4522(84)90195-7.

Basu, R., Duan, X., Taylor, M. R., Martin, E. A., Muralidhar, S., Wang, Y., et al. (2017). Heterophilic Type II Cadherins Are Required for High-Magnitude Synaptic Potentiation in the Hippocampus. *Neuron* 96, 160-176.e8. doi:10.1016/j.neuron.2017.09.009.
Basu, R., Taylor, M. R., and Williams, M. E. (2015). The classic cadherins in synaptic specificity. *Cell Adhesion & Migration* 9, 193–201. doi:10.1080/19336918.2014.1000072.
Briggman, K. L., Helmstaedter, M., and Denk, W. (2011). Wiring specificity in the direction-selectivity circuit of the retina. *Nature* 471, 183–188. doi:10.1038/nature09818.
Buffelli, M., Burgess, R. W., Feng, G., Lobe, C. G., Lichtman, J. W., and Sanes, J. R. (2003). Genetic evidence that relative synaptic efficacy biases the outcome of synaptic competition. *Nature* 424, 430–434. doi:10.1038/nature01844.
Carter-Dawson, L. D., and Lavail, M. M. (1979). Rods and cones in the mouse retina. II. Autoradiographic analysis of cell generation using tritiated thymidine. *Journal of Comparative Neurology* 188, 263–272. doi:10.1002/cne.901880205.
Centanin, L., and Wittbrodt, J. (2014). Retinal neurogenesis. *Development* 141, 241–244. doi:10.1242/dev.083642.
Cepko, C. L., Austin, C. P., Yang, X., Alexiades, M., and Ezzeddine, D. (1996). Cell fate determination in the vertebrate retina. *Proc Natl Acad Sci U S A* 93, 589–595.
Chalupa, L. M., and Günhan, E. (2004). Development of On and Off retinal pathways and retinogeniculate projections. *Progress in Retinal and Eye Research* 23, 31–51. doi:10.1016/j.preteyeres.2003.10.001.
Chen, T.-W., Wardill, T. J., Sun, Y., Pulver, S. R., Renninger, S. L., Baohan, A., et al. (2013). Ultrasensitive fluorescent proteins for imaging neuronal activity. *Nature* 499, 295–300. doi:10.1038/nature12354.
Cook, J. E., and Chalupa, L. M. (2000). Retinal mosaics: new insights into an old concept. *Trends in Neurosciences* 23, 26–34. doi:10.1016/S0166-2236(99)01487-3.
Deans, M. R., Krol, A., Abraira, V. E., Copley, C. O., Tucker, A. F., and Goodrich, L. V. (2011). Control of neuronal morphology by the atypical cadherin Fat3. *Neuron* 71, 820–832. doi:10.1016/j.neuron.2011.06.026.
Demb, J. B., and Singer, J. H. (2015). Functional Circuitry of the Retina. *Annual Review of Vision Science* 1, 263–289. doi:10.1146/annurev-vision-082114-035334.
Dhande, O. S., Estevez, M. E., Quattrochi, L. E., El-Danaf, R. N., Nguyen, P. L., Berson, D. M., et al. (2013). Genetic dissection of retinal inputs to brainstem nuclei controlling image stabilization. *J. Neurosci.* 33, 17797–17813. doi:10.1523/JNEUROSCI.2778-13.2013.
Diamond, J. S. (2017). Inhibitory Interneurons in the Retina: Types, Circuitry, and Function. *Annual Review of Vision Science* 3, 1–24. doi:10.1146/annurev-vision-102016-061345.
Duan, X., Krishnaswamy, A., De la Huerta, I., and Sanes, J. R. (2014). Type II cadherins guide assembly of a direction-selective retinal circuit. *Cell* 158, 793–807. doi:10.1016/j.cell.2014.06.047.
Duan, X., Krishnaswamy, A., Laboulaye, M. A., Liu, J., Peng, Y.-R., Yamagata, M., et al. (2018). Cadherin Combinations Recruit Dendrites of Distinct Retinal Neurons to a Shared Interneuronal Scaffold. *Neuron* 99, 1145-1154.e6. doi:10.1016/j.neuron.2018.08.019.
Euler, T., Hausselt, S. E., Margolis, D. J., Breuninger, T., Castell, X., Detwiler, P. B., et al. (2009). Eyecup scope—optical recordings of light stimulus-evoked fluorescence signals in the retina. *Pflugers Arch - Eur J Physiol* 457, 1393–1414. doi:10.1007/s00424-008-0603-5.

Euler, T., Haverkamp, S., Schubert, T., and Baden, T. (2014). Retinal bipolar cells: elementary building blocks of vision. *Nat Rev Neurosci* 15, 507–519. doi:10.1038/nrn3783.
Field, G. D., Sher, A., Gauthier, J. L., Greschner, M., Shlens, J., Litke, A. M., et al. (2007). Spatial Properties and Functional Organization of Small Bistratified Ganglion Cells in Primate Retina. *J Neurosci* 27, 13261–13272. doi:10.1523/JNEUROSCI.3437-07.2007.
Fu, Y., and Yau, K.-W. (2007). Phototransduction in mouse rods and cones. *Pflugers Arch* 454, 805–819. doi:10.1007/s00424-006-0194-y.
Fuerst, P. G., Bruce, F., Tian, M., Wei, W., Elstrott, J., Feller, M. B., et al. (2009). DSCAM and DSCAML1 function in self-avoidance in multiple cell types in the developing mouse retina. *Neuron* 64, 484–97. doi:10.1016/j.neuron.2009.09.027.
Gollisch, T., and Meister, M. (2010). Eye Smarter than Scientists Believed: Neural Computations in Circuits of the Retina. *Neuron* 65, 150–164. doi:10.1016/j.neuron.2009.12.009.
Hatta, K., Takagi, S., Fujisawa, H., and Takeichi, M. (1987). Spatial and temporal expression pattern of N-cadherin cell adhesion molecules correlated with morphogenetic processes of chicken embryos. *Dev. Biol.* 120, 215–227. doi:10.1016/0012-1606(87)90119-9.
Helmstaedter, M., Briggman, K. L., Turaga, S. C., Jain, V., Seung, H. S., and Denk, W. (2013). Connectomic reconstruction of the inner plexiform layer in the mouse retina. *Nature* 500, 168–174. doi:10.1038/nature12346.
Hsiang, J.-C., Johnson, K. P., Madisen, L., Zeng, H., and Kerschensteiner, D. (2017). Local processing in neurites of VGluT3-expressing amacrine cells differentially organizes visual information. *eLife* 6, e31307. doi:10.7554/eLife.31307.
Hubel, D. H. (1959). Single unit activity in striate cortex of unrestrained cats. *J Physiol* 147, 226-238.2.
Huber, A. B., Kolodkin, A. L., Ginty, D. D., and Cloutier, J.-F. (2003). Signaling at the growth cone: ligand-receptor complexes and the control of axon growth and guidance. *Annu. Rev. Neurosci.* 26, 509–563. doi:10.1146/annurev.neuro.26.010302.081139.
Inoue, T., Tanaka, T., Suzuki, S. C., and Takeichi, M. (1998). Cadherin-6 in the developing mouse brain: expression along restricted connection systems and synaptic localization suggest a potential role in neuronal circuitry. *Dev. Dyn.* 211, 338–351. doi:10.1002/(SICI)1097-0177(199804)211:4<338::AID-AJA5>3.0.CO;2-I.
Inuzuka, H., Miyatani, S., and Takeichi, M. (1991). R-cadherin: A novel Ca2+-dependent cell-cell adhesion molecule expressed in the retina. *Neuron* 7, 69–79. doi:10.1016/0896-6273(91)90075-B.
JN., L. (1892). On the origin from the spinal cord of the cervical and upper thoracic sympathetic fibres, with some observations on white and grey rami communications. *Philos. Trans. R. Soc. London* B, 85–124.
Johnson, J., Sherry, D. M., Liu, X., Fremeau, R. T., Seal, R. P., Edwards, R. H., et al. (2004). Vesicular glutamate transporter 3 expression identifies glutamatergic amacrine cells in the rodent retina. *Journal of Comparative Neurology* 477, 386–398. doi:10.1002/cne.20250.
Karten, H. J., and Brecha, N. (1983). Localization of neuroactive substances in the vertebrate retina: Evidence for lamination in the inner plexiform layer. *Vision Research* 23, 1197–1205. doi:10.1016/0042-6989(83)90033-0.
Kay, J. N., De la Huerta, I., Kim, I.-J., Zhang, Y., Yamagata, M., Chu, M. W., et al. (2011). Retinal Ganglion Cells with Distinct Directional Preferences Differ in Molecular Identity,

Structure, and Central Projections. *J Neurosci* 31, 7753–7762. doi:10.1523/JNEUROSCI.0907-11.2011.
Kim, I.-J., Zhang, Y., Yamagata, M., Meister, M., and Sanes, J. R. (2008). Molecular identification of a retinal cell type that responds to upward motion. *Nature* 452, 478–482. doi:10.1038/nature06739.
Kim, T., and Kerschensteiner, D. (2017). Inhibitory Control of Feature Selectivity in an Object Motion Sensitive Circuit of the Retina. *Cell Reports* 19, 1343–1350. doi:10.1016/j.celrep.2017.04.060.
Kim, T., Soto, F., and Kerschensteiner, D. (2015). An excitatory amacrine cell detects object motion and provides feature-selective input to ganglion cells in the mouse retina. *Elife* 4. doi:10.7554/eLife.08025.
Koike, C., Numata, T., Ueda, H., Mori, Y., and Furukawa, T. (2010a). TRPM1: A vertebrate TRP channel responsible for retinal ON bipolar function. *Cell Calcium* 48, 95–101. doi:10.1016/j.ceca.2010.08.004.
Koike, C., Obara, T., Uriu, Y., Numata, T., Sanuki, R., Miyata, K., et al. (2010b). TRPM1 is a component of the retinal ON bipolar cell transduction channel in the mGluR6 cascade. *Proceedings of the National Academy of Sciences* 107, 332–337. doi:10.1073/pnas.0912730107.
Koropouli, E., and Kolodkin, A. L. (2014). Semaphorins and the dynamic regulation of synapse assembly, refinement, and function. *Current Opinion in Neurobiology* 27, 1–7. doi:10.1016/j.conb.2014.02.005.
Krieger, B., Qiao, M., Rousso, D. L., Sanes, J. R., and Meister, M. (2017). Four alpha ganglion cell types in mouse retina: Function, structure, and molecular signatures. *PLOS ONE* 12, e0180091. doi:10.1371/journal.pone.0180091.
Krishnaswamy, A., Yamagata, M., Duan, X., Hong, Y. K., and Sanes, J. R. (2015). Sidekick 2 directs formation of a retinal circuit that detects differential motion. *Nature* 524, 466–470. doi:10.1038/nature14682.
Laboissonniere, L. A., Goetz, J. J., Martin, G. M., Bi, R., Lund, T. J. S., Ellson, L., et al. (2019). Molecular signatures of retinal ganglion cells revealed through single cell profiling. *Scientific Reports* 9, 1–15. doi:10.1038/s41598-019-52215-4.
Lagnado, L., and Baylor, D. (1992). Signal flow in visual transduction. *Neuron* 8, 995–1002. doi:10.1016/0896-6273(92)90122-T.
Lee, S., Chen, L., Chen, M., Ye, M., Seal, R. P., and Zhou, Z. J. (2014). An Unconventional Glutamatergic Circuit in the Retina Formed by vGluT3 Amacrine Cells. *Neuron* 84, 708–715. doi:10.1016/j.neuron.2014.10.021.
Lefebvre, J. L., Kostadinov, D., Chen, W. V., Maniatis, T., and Sanes, J. R. (2012). Protocadherins mediate dendritic self-avoidance in the mammalian nervous system. *Nature* 488, 517–21. doi:10.1038/nature11305.
Lefebvre, J. L., Sanes, J. R., and Kay, J. N. (2015). Development of dendritic form and function. *Annu. Rev. Cell Dev. Biol.* 31, 741–777. doi:10.1146/annurev-cellbio-100913-013020.
Liu, J., Reggiani, J. D. S., Laboulaye, M. A., Pandey, S., Chen, B., Rubenstein, J. L. R., et al. (2018). Tbr1 instructs laminar patterning of retinal ganglion cell dendrites. *Nat Neurosci* 21, 659–670. doi:10.1038/s41593-018-0127-z.

Lolley, R. N., and Lee, R. H. (1990). Cyclic GMP and photoreceptor function. *The FASEB Journal* 4, 3001–3008. doi:10.1096/fasebj.4.12.1697545.
Luo, D.-G., and Yau, K.-W. (2005). Rod Sensitivity of Neonatal Mouse and Rat. *J Gen Physiol* 126, 263–269. doi:10.1085/jgp.200509342.
MacNeil, M. A., and Masland, R. H. (1998). Extreme Diversity among Amacrine Cells: Implications for Function. *Neuron* 20, 971–982. doi:10.1016/S0896-6273(00)80478-X.
Macosko, E. Z., Basu, A., Satija, R., Nemesh, J., Shekhar, K., Goldman, M., et al. (2015). Highly Parallel Genome-wide Expression Profiling of Individual Cells Using Nanoliter Droplets. *Cell* 161, 1202–1214. doi:10.1016/j.cell.2015.05.002.
Marquardt, T., and Gruss, P. (2002). Generating neuronal diversity in the retina: one for nearly all. *Trends in Neurosciences* 25, 32–38. doi:10.1016/S0166-2236(00)02028-2.
Martersteck, E. M., Hirokawa, K. E., Evarts, M., Bernard, A., Duan, X., Li, Y., et al. (2017). Diverse Central Projection Patterns of Retinal Ganglion Cells. *Cell Reports* 18, 2058–2072. doi:10.1016/j.celrep.2017.01.075.
Masland, R. H. (2012a). The Neuronal Organization of the Retina. *Neuron* 76, 266–280. doi:10.1016/j.neuron.2012.10.002.
Masland, R. H. (2012b). The tasks of amacrine cells. *Vis Neurosci* 29, 3–9.
Matsuoka, R. L., Chivatakarn, O., Badea, T. C., Samuels, I. S., Cahill, H., Katayama, K.-I., et al. (2011a). Class 5 transmembrane semaphorins control selective Mammalian retinal lamination and function. *Neuron* 71, 460–473. doi:10.1016/j.neuron.2011.06.009.
Matsuoka, R. L., Nguyen-Ba-Charvet, K. T., Parray, A., Badea, T. C., Chedotal, A., and Kolodkin, A. L. (2011b). Transmembrane semaphorin signalling controls laminar stratification in the mammalian retina. *Nature* 470, 259–63. doi:10.1038/nature09675.
Matsuoka, R. L., Sun, L. O., Katayama, K., Yoshida, Y., and Kolodkin, A. L. (2013). Sema6B, Sema6C, and Sema6D expression and function during mammalian retinal development. *PLoS ONE* 8, e63207. doi:10.1371/journal.pone.0063207.
Miskevich, F., Zhu, Y., Ranscht, B., and Sanes, J. R. (1998). Expression of multiple cadherins and catenins in the chick optic tectum. *Mol. Cell. Neurosci.* 12, 240–255. doi:10.1006/mcne.1998.0718.
Molnar, A., Hsueh, H.-A., Roska, B., and Werblin, F. S. (2009). Crossover inhibition in the retina: circuitry that compensates for nonlinear rectifying synaptic transmission. *J Comput Neurosci* 27, 569–590. doi:10.1007/s10827-009-0170-6.
Nguyen-Ba-Charvet, K. T., and Rebsam, A. (2020). Neurogenesis and Specification of Retinal Ganglion Cells. *International Journal of Molecular Sciences* 21, 451. doi:10.3390/ijms21020451.
Nikonov, S. S., Kholodenko, R., Lem, J., and Pugh, E. N. (2006). Physiological Features of the S- and M-cone Photoreceptors of Wild-type Mice from Single-cell Recordings. *J Gen Physiol* 127, 359–374. doi:10.1085/jgp.200609490.
Oberst, P., Agirman, G., and Jabaudon, D. (2019). Principles of progenitor temporal patterning in the developing invertebrate and vertebrate nervous system. *Current Opinion in Neurobiology* 56, 185–193. doi:10.1016/j.conb.2019.03.004.
Ölveczky, B. P., Baccus, S. A., and Meister, M. (2007). Retinal Adaptation to Object Motion. *Neuron* 56, 689–700. doi:10.1016/j.neuron.2007.09.030.

Peichl, L., and González-Soriano, J. (1994). Morphological types of horizontal cell in rodent retinae: a comparison of rat, mouse, gerbil, and guinea pig. *Vis. Neurosci.* 11, 501–517. doi:10.1017/s095252380000242x.
Porrero, C., Rubio-Garrido, P., Avendaño, C., and Clascá, F. (2010). Mapping of fluorescent protein-expressing neurons and axon pathways in adult and developing Thy1-eYFP-H transgenic mice. *Brain Res.* 1345, 59–72. doi:10.1016/j.brainres.2010.05.061.
Ray, T. A., Roy, S., Kozlowski, C., Wang, J., Cafaro, J., Hulbert, S. W., et al. (2018). Formation of retinal direction-selective circuitry initiated by starburst amacrine cell homotypic contact. *Elife* 7. doi:10.7554/eLife.34241.
Raymond, I. D., Vila, A., Huynh, U.-C. N., and Brecha, N. C. (2008). Cyan fluorescent protein expression in ganglion and amacrine cells in a thy1-CFP transgenic mouse retina. *Mol Vis* 14, 1559–1574.
Redies, C. (2000). Cadherins in the central nervous system. *Progress in Neurobiology* 61, 611–648. doi:10.1016/S0301-0082(99)00070-2.
Reese, B. E., and Galli-Resta, L. (2002). The role of tangential dispersion in retinal mosaic formation. *Progress in Retinal and Eye Research* 21, 153–168. doi:10.1016/S1350-9462(01)00024-6.
Rheaume, B. A., Jereen, A., Bolisetty, M., Sajid, M. S., Yang, Y., Renna, K., et al. (2018). Single cell transcriptome profiling of retinal ganglion cells identifies cellular subtypes. *Nat Commun* 9, 1–17. doi:10.1038/s41467-018-05134-3.
Riccomagno, M. M., Sun, L. O., Brady, C. M., Alexandropoulos, K., Seo, S., Kurokawa, M., et al. (2014). Cas Adaptor Proteins Organize the Retinal Ganglion Cell Layer Downstream of Integrin Signaling. *Neuron* 81, 779–786. doi:10.1016/j.neuron.2014.01.036.
Rodieck, R. W., and Marshak, D. W. (1992). Spatial density and distribution of choline acetyltransferase immunoreactive cells in human, macaque, and baboon retinas. *Journal of Comparative Neurology* 321, 46–64. doi:10.1002/cne.903210106.
Rousso, D. L., Qiao, M., Kagan, R. D., Yamagata, M., Palmiter, R. D., and Sanes, J. R. (2016). Two pairs of ON and OFF retinal ganglion cells are defined by intersectional patterns of transcription factor expression. *Cell Rep* 15, 1930–1944. doi:10.1016/j.celrep.2016.04.069.
Sanes, J. R., and Masland, R. H. (2015). The Types of Retinal Ganglion Cells: Current Status and Implications for Neuronal Classification. *Annu. Rev. Neurosci.* 38, 221–246. doi:10.1146/annurev-neuro-071714-034120.
Sanes, J. R., and Yamagata, M. (1999). Formation of lamina-specific synaptic connections. *Current Opinion in Neurobiology* 9, 79–87. doi:10.1016/S0959-4388(99)80010-5.
Sanes, J. R., and Yamagata, M. (2009). Many paths to synaptic specificity. *Annu. Rev. Cell Dev. Biol.* 25, 161–195. doi:10.1146/annurev.cellbio.24.110707.175402.
Sanes, J. R., and Zipursky, S. L. (2010). Design Principles of Insect and Vertebrate Visual Systems. *Neuron* 66, 15–36. doi:10.1016/j.neuron.2010.01.018.
Seabrook, T. A., Burbridge, T. J., Crair, M. C., and Huberman, A. D. (2017). Architecture, Function, and Assembly of the Mouse Visual System. *Annu. Rev. Neurosci.* 40, 499–538. doi:10.1146/annurev-neuro-071714-033842.
Shekhar, K., Lapan, S. W., Whitney, I. E., Tran, N. M., Macosko, E. Z., Kowalczyk, M., et al. (2016). Comprehensive Classification of Retinal Bipolar Neurons by Single-Cell Transcriptomics. *Cell* 166, 1308-1323.e30. doi:10.1016/j.cell.2016.07.054.

Shi, Q., Gupta, P., Boukhvalova, A. K., Singer, J. H., and Butts, D. A. (2019). Functional characterization of retinal ganglion cells using tailored nonlinear modeling. *Scientific Reports* 9, 1–12. doi:10.1038/s41598-019-45048-8.
Shimoyama, Y., Tsujimoto, G., Kitajima, M., and Natori, M. (2000). Identification of three human type-II classic cadherins and frequent heterophilic interactions between different subclasses of type-II classic cadherins. *Biochem. J.* 349, 159–167. doi:10.1042/0264-6021:3490159.
Sperry, R. W. (1943). Visuomotor coordination in the newt (Triturus viridescens) after regeneration of the optic nerve. *J Comp Neurol* 79, 33–55. doi:10.1002/cne.900790104.
Stacy, R. C., and Wong, R. O. L. (2003). Developmental relationship between cholinergic amacrine cell processes and ganglion cell dendrites of the mouse retina. *J. Comp. Neurol.* 456, 154–166. doi:10.1002/cne.10509.
Sterling, P., Smith, R. G., Rao, R., and Vardi, N. (1995). “Functional architecture of mammalian outer retina and bipolar cells,” in *Neurobiology and Clinical Aspects of the Outer Retina*, eds. M. B. A. Djamgoz, S. N. Archer, and S. Vallerga (Dordrecht: Springer Netherlands), 325–348. doi:10.1007/978-94-011-0533-0_13.
Sun, L. O., Jiang, Z., Rivlin-Etzion, M., Hand, R., Brady, C. M., Matsuoka, R. L., et al. (2013). On and off retinal circuit assembly by divergent molecular mechanisms. *Science* 342, 1241974. doi:10.1126/science.1241974.
Suzuki, S. C., Inoue, T., Kimura, Y., Tanaka, T., and Takeichi, M. (1997). Neuronal circuits are subdivided by differential expression of type-II classic cadherins in postnatal mouse brains. *Mol. Cell. Neurosci.* 9, 433–447. doi:10.1006/mcne.1997.0626.
Suzuki, S., Sano, K., and Tanihara, H. (1991). Diversity of the cadherin family: evidence for eight new cadherins in nervous tissue. *Cell Regul.* 2, 261–270.
Takeichi, M. (1988). The cadherins: cell-cell adhesion molecules controlling animal morphogenesis. *Development* 102, 639–655.
Tan, L., Zhang, K. X., Pecot, M. Y., Nagarkar-Jaiswal, S., Lee, P.-T., Takemura, S.-Y., et al. (2015). Ig Superfamily Ligand and Receptor Pairs Expressed in Synaptic Partners in Drosophila. *Cell* 163, 1756–1769. doi:10.1016/j.cell.2015.11.021.
Thoreson, W. B., and Mangel, S. C. (2012). Lateral interactions in the outer retina. *Progress in Retinal and Eye Research* 31, 407–441. doi:10.1016/j.preteyeres.2012.04.003.
Tran, N. M., Shekhar, K., Whitney, I. E., Jacobi, A., Benhar, I., Hong, G., et al. (2019). Single-Cell Profiles of Retinal Ganglion Cells Differing in Resilience to Injury Reveal Neuroprotective Genes. *Neuron* 104, 1039-1055.e12. doi:10.1016/j.neuron.2019.11.006.
Turner, M. H., Schwartz, G. W., and Rieke, F. (2018). Receptive field center-surround interactions mediate context-dependent spatial contrast encoding in the retina. *eLife* 7, e38841. doi:10.7554/eLife.38841.
Twig, G., Levy, H., and Perlman, I. (2003). Color opponency in horizontal cells of the vertebrate retina. *Progress in Retinal and Eye Research* 22, 31–68. doi:10.1016/S1350-9462(02)00045-9.
Voinescu, P. E., Kay, J. N., and Sanes, J. R. (2009). Birthdays of retinal amacrine cell subtypes are systematically related to their molecular identity and soma position. *Journal of Comparative Neurology* 517, 737–750. doi:10.1002/cne.22200.
Wei, W., Hamby, A. M., Zhou, K., and Feller, M. B. (2011). Development of asymmetric inhibition underlying direction selectivity in the retina. *Nature* 469, 402–6. doi:10.1038/nature09600.

Werblin, F. S. (2011). The retinal hypercircuit: a repeating synaptic interactive motif underlying visual function. *The Journal of Physiology* 589, 3691–3702. doi:10.1113/jphysiol.2011.210617.
Werblin, F. S., and Dowling, J. E. (1969). Organization of the retina of the mudpuppy, Necturus maculosus. II. Intracellular recording. *Journal of Neurophysiology* 32, 339–355. doi:10.1152/jn.1969.32.3.339.
Williams, M. E., de Wit, J., and Ghosh, A. (2010). Molecular Mechanisms of Synaptic Specificity in Developing Neural Circuits. *Neuron* 68, 9–18. doi:10.1016/j.neuron.2010.09.007.
Williams, M. E., Wilke, S. A., Daggett, A., Davis, E., Otto, S., Ravi, D., et al. (2011). Cadherin-9 regulates synapse-specific differentiation in the developing hippocampus. *Neuron* 71, 640–55. doi:10.1016/j.neuron.2011.06.019.
Xu, S., Xiao, Q., Cosmanescu, F., Sergeeva, A. P., Yoo, J., Lin, Y., et al. (2018). Interactions between the Ig-Superfamily Proteins DIP-α and Dpr6/10 Regulate Assembly of Neural Circuits. *Neuron* 100, 1369-1384.e6. doi:10.1016/j.neuron.2018.11.001.
y Cajal Santiago Ramón (1972). *The structure of the retina*. Charles C. Thomas Publisher.
Yan, W., Laboulaye, M. A., Tran, N. M., Whitney, I. E., Benhar, I., and Sanes, J. R. (2020). Molecular identification of sixty-three amacrine cell types completes a mouse retinal cell atlas. *bioRxiv*, 2020.03.10.985770. doi:10.1101/2020.03.10.985770.
Yang, X. L., and Wu, S. M. (1991). Feedforward lateral inhibition in retinal bipolar cells: input-output relation of the horizontal cell-depolarizing bipolar cell synapse. *Proc Natl Acad Sci U S A* 88, 3310–3313.
Yonehara, K., Balint, K., Noda, M., Nagel, G., Bamberg, E., and Roska, B. (2011). Spatially asymmetric reorganization of inhibition establishes a motion-sensitive circuit. *Nature* 469, 407–410. doi:10.1038/nature09711.
Yoshida, K., Watanabe, D., Ishikane, H., Tachibana, M., Pastan, I., and Nakanishi, S. (2001). A key role of starburst amacrine cells in originating retinal directional selectivity and optokinetic eye movement. *Neuron* 30, 771–780. doi:10.1016/s0896-6273(01)00316-6.
Young, R. W. (1985). Cell differentiation in the retina of the mouse. *Anat. Rec.* 212, 199–205. doi:10.1002/ar.1092120215.
Zhang, A.-J., Zhang, J., and Wu, S. M. (2006a). Electrical coupling, receptive fields, and relative rod/cone inputs of horizontal cells in the tiger salamander retina. *Journal of Comparative Neurology* 499, 422–431. doi:10.1002/cne.21117.
Zhang, C., Kolodkin, A. L., Wong, R. O., and James, R. E. (2017). Establishing Wiring Specificity in Visual System Circuits: From the Retina to the Brain. *Annu. Rev. Neurosci.* 40, 395–424. doi:10.1146/annurev-neuro-072116-031607.
Zhang, J., Li, W., Hoshi, H., Mills, S. L., and Massey, S. C. (2005). Stratification of alpha ganglion cells and ON/OFF directionally selective ganglion cells in the rabbit retina. *Vis Neurosci* 22, 535–549. doi:10.1017/S0952523805224148.
Zhang, J., Zhang, A.-J., and Wu, S. M. (2006b). Immunocytochemical analysis of GABA-positive and calretinin-positive horizontal cells in the tiger salamander retina. *Journal of Comparative Neurology* 499, 432–441. doi:10.1002/cne.21116.
Zipursky, S. L., and Sanes, J. R. (2010). Chemoaffinity revisited: dscams, protocadherins, and neural circuit assembly. *Cell* 143, 343–353. doi:10.1016/j.cell.2010.10.009.